UNIVERSITAT DE BARCELONA

Facultat de Matemàtiques
i Informàtica

GRAU DE MATEMÀTIQUES

Treball final de grau

The Hodgkin-Huxley and simpler models. Bursting behaviour.

Autor: Alexandra Pairó López

Director: Dr. Arturo Vieiro Yanes
Realitzat a: Departament de sistemes dinàmics

Barcelona, 24 de gener de 2022

Abstract

The main goal of this work is to understand the best model for describing neuronal activity, the Hodgkin-Huxley model, doing simulations of it and studying simpler models that are able to display some of the Hodgkin-Huxley activity. We are going to study FitzHugh-Nagumo, Morris-Lecar and Hindmarsh-Rose model. In addition, since we want to study neuron activity via dynamical systems, we also study bursting behaviour. We want to understand how different kinds of bifurcations in dynamical systems affect neuron activity, studying the bifurcations that take part in such activity.

Acknowledgement

I would like to express my deep and sincere gratitude to my tutor, Arturo Vieiro Yanes, who has advised me and helped me through all this work.

Secondly, I would like to thank my parents, my sister and my friends for being always there for me during this journey and all these years. I will always be overwhelmed by the support I have always received.

2020 Mathematics Subject Classification. 37-00, 37-02, 37-11

Contents

Introduction

Mathematics in neuroscience permits another insight into the activity of neurons, leading to a wide range of discoveries and improvements. The relation between neuroscience and dynamical systems provides you with more information about how neurons communicate. In neuronal activity, the major phenomena that occur are resting or quiescent, action potential or spiking, chaotic behaviour and bursting, all of them covered in this project.

In the first chapter, we introduce the more famous and quintessential model that describes neurons dynamics: the Hodgkin-Huxley model. Since it is a four-dimensional model, it is a difficult model to analyze. This caused the emergence of simpler models that displayed some neuron activity that resembles the one exhibited by the Hodgkin-Huxley. In this project, we are going to see FitzHugh-Nagumo, Morris-Lecar and Hindmarsh-Rose model.

In the next chapter, we are going to study the FitzHugh-Nagumo model, which is a simpler model that does not take into account the biological information of neurons focusing exclusively on the mathematical properties. We are going to focus on periodic neurons' activity, doing simulations of such activity integrating the equations of the model.

The last chapter introduces an important phenomenon in neuronal communication that allows the transmission of more information between neurons: bursting excitability. We are going to simulate such phenomena integrating Morris-Lecar and Hindmarsh-Rose model. Those models are fast-slow models with a one-dimensional slow variable. Such underlying structure of the models is essential to create the bifurcation sequences leading to bursting.

In the end, we include a brief summary and conclusions of the work adding some future work we could consider.

Chapter 1

Hodgkin and Huxley Model

1.1 Previous Content

Alan Lloyd Hodgkin and Andrew Huxley [16] are well-known for their studies on bifurcations in neuronal models, being the first ones to relate bifurcations on dynamical systems to neuroscience and creating the most accepted model to describe neurons kinetics. Neuronal models provide information about how neurons interact, how information is transmitted through them. The connection between mathematics and neuroscience leads to a wide range of discoveries, such as the computations of neurons.

Hodgkin-Huxley model is the most important model computed by Hodgkin and Huxley in 1952 studying the axon of a squid, chosen because of its hugeness compared to other neurons. They studied the different changes in membrane voltage that the cell undergoes, applying different amplitudes of currents experimentally focusing on the abrupt changes of the membrane voltage, similarly called action potentials or spikes. An action potential is an abrupt and transient change of resting membrane voltage or resting membrane potential, this spike is perceived by other cells and is their communication media. The cell membrane can be depolarized, the membrane voltage can become more positive; it can be hyperpolarized, the membrane potential goes far away from the resting state in a negative way; and repolarized, the membrane voltage lows until the resting state is achieved. The model wanted to study the generation and propagation of an action potential.

The model was issued from studying the neuron as an electric circuit and applying all the properties known there. Firstly, they observed that the membrane had an associated electric capacitance and an electric potential difference between

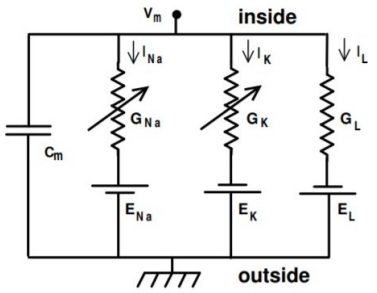

Figure 1.1: Equivalent circuit proposed by Hodgkin and Huxley. Figure taken from [4].

the inside and the outside of the cell, being the inside negative over the exterior.

Definition 1.1. *An ion is a charged atom, i.e. an atom that loses or gains one or more electrons. Ion channels are macromolecular pores located in all cells membranes that are constantly opening and closing to signals and responses.*

Ion channels play an important role in the excitability of nerve and muscle, as they have as main function to establish a resting membrane potential. In addition, each channel is like an excitable molecule because it responds to some stimulus such as membrane potential changes, other chemical stimulus, synapses[1]... Hence, the cell membrane needs to be studied as a circuit containing the conductance of the currents[2], i.e. the ability of an ion to fluctuate across the cell membrane, and the membrane capacitance. As not all ions are allowed to flow in and out and the membrane can be permeable or impermeable to some kind of ions, a membrane capacitance is utterly necessary.

Definition 1.2. *Gating is the opening or closing of the pore when the channel responds to stimulus. A gate is a channel capable of gating.*

There are a lot of ions that take part in biological procedure in human body, some of them are H^+, Mg^{2+}, Cl^-, Na^+, K^+, Ca^{2+}, HCO_3^- and HPO_4^{2-}. When it comes to the nervous system, Na^+, K^+, Ca^{2+} and Cl^- are the main responsible for the action. The giant axon has three major currents: persistent outward K^+ current with four activation gates, transient inward Na^+ current with one inactivation gate and three activation gates, and a leak current mostly carried by Cl^- ions experimentally. Inward Na^+ current depolarizes the membrane potential and outward K^+ current hyperpolarizes it. The leak current is constant and it does not depend on the conductance, so it does not have activation and inactivation variables as the other ones do. Moreover, on cell membranes, there are places where

[1] A synapse is a connection between neurons.

[2] A current is any net flow of charges.

the current flows naturally and we cannot control it, which is why we consider the leaky current.

Experimentally, Hodgkin and Huxley applied two different techniques: space clamp or voltage-clamp. The space clamp technique consists of preserving a uniform spatial distribution of the membrane current, removing the spatial dependence. Hence, having an ordinary differential equation. The voltage-clamp technique consists of maintaining the voltage of the membrane at a desired value.

1.2 Background of the equations

The net current of an ion, using Ohm's law[3], is $V = IR$ and the conductance of the membrane is given by $g = 1/R$, where R is the membrane resistance, V is the potential difference and I is the intensity current, being R, V and, in consequence, I different for each kind of ion. Hence, the size of the current is determined by two factors: the potential difference and the electrical conductance. Joining the prior, we get the expression of the intensity for each ion: $I_{ion} = g_{ion} V_{ion}$.

Definition 1.3. *[24] The conductance, g, is the ease of flow of current between two points. The resistance is the reciprocal of the conductance.*

Definition 1.4. *[24] The potential difference, V, is the work needed to move a unit test charge in a frictionless manner from one point to another.*

Definition 1.5. *Nernst equilibrium potential value[4] is a potential value for which the current flowing through the membrane stabilizes and equals 0, i.e. net crossing membrane is 0. Due to the depolarizing and hyperpolarizing of the membrane, its goal is to stabilize itself reaching an equilibrium called Nernst equilibrium. The Nernst equilibrium is given by the expression proposed by Walter Nernst:*

$$E_{ion} = \frac{R^* T}{zF} \ln\left(\frac{[Ion]_{out}}{[Ion]_{in}}\right),$$

where T is the temperature in Kelvins, F is the Faraday's constant, R^* is the universal gas constant, z is the valence[4] of the ion, $[Ion]_{in}$ is the concentration of the ion inside the cell and $[Ion]_{out}$ is the concentration of the ion outside the cell.

[3]The Ohm's law states that the current through an electric circuit between two points is directly proportional to the voltage across such two points. The constant of proportionality is the resistance of the circuit. Hence, we arrive at the mathematical expression: $I = V/R$.

[4]Valence of an ion is the combining capacity with other atoms when forming molecules or chemical elements. For example, if an atom has valence 1 it can be combined with only one atom.

In the model, V_{ion} is called the driving force and is considered $V - E_{ion}$ where E_{ion} is the ion's Nernst equilibrium potential, which depends on every ion, and V is the global membrane voltage. The driving force is the difference between the global membrane voltage and the Nernst equilibrium. In a current of ions, the voltage needs to be considered $V - E_{ion}$ because the current will be inward or outward depending on the Nernst equilibrium. We will have more or less intensity of a current of an ion if the global membrane voltage is further or closer to the Nernst equilibrium of such ion. We will have an inward or outward current if the membrane voltage is bigger or lower than the Nernst equilibrium. For example, when the sodium concentration is bigger than its equilibrium, the current is inward. In conclusion, the intensity of the current of ions is

$$I_{ion} = g_{ion}(V - E_{ion}), \tag{1.1}$$

being the conductance of an ion, g_{ion}, not constant on channels because there is a transient inflow or outflow of them and the Nernst equilibrium potential, E_{ion}, constant although it can hold different values in different experiments.

Furthermore, the intensity of a current is the instant change of charge: $I_c = \frac{dq}{dt}$, where I_c in the model is the intensity current of the membrane, which has been studied as an electric circuit, and q the charge of the current. The charge is related to the capacitance of the membrane, Cm[5], and the global voltage membrane, V, having $q = C_m V$. Deriving with respect to time, we get $\frac{dq}{dt} = C_m \frac{dV}{dt} = I_c$. In consequence, using First Kirchhoff's law[6] and considering that the total current that travels through the membrane is formed by the intensity current of the membrane, I_c, and the intensity current of the ions, I_{ions}, we have the expression:

$$I_c + I_{ions} = 0, \tag{1.2}$$

and $I_c = C_m \frac{\partial V}{\partial t} = -I_{ions}$.

When we have an external current, carried out by synapses or applied experimentally, the sum of (1.2) equals the intensity of the applied current, i.e. $I_{ext} = I_c + I_{ions}$, where $I_{ions} = \sum_k g_k(V - E_k)$, where k ranges over the finite set of ions we have.

[5]The membrane capacitance, C_m, is considered constant in order to simplify experiments and research.

[6]The first Kirchhoff's law states that the sum of all intensities inside a circuit equals 0 if no external current is applied, i.e. in a circuit point the sum of all inward currents equals the sum of all outward currents.

The behaviour of an electric current can be described by the equations: $C_m \frac{dV}{dt} + I_{ion} = I_{ext}$. A positive external current, i.e. $I_{ext} > 0$, will tend to depolarize the cell, whereas a positive ionic current, i.e. $I_{ion} > 0$, will hyperpolarize the cell. Taken into account the different ions on the squid axon, we get the equation that expresses the change in the membrane voltage according to the different channels

$$C_m \dot{V} = I_{ext} - I_K - I_{Na} - I_L, \tag{1.3}$$

being $\dot{V} = \frac{dV}{dt}$.

When it comes to the net current of an ion on a channel, we have to take into account that the conductance is a time and voltage-dependent function. According to the creation of an action potential, we can see how the flow of each ion changes over time and voltage. Voltage sensors located on the membrane open an activation gate and allow selected ions to flow through the channels or open an inactivation gate that blocks the channel. That is why g for transient ions currents is defined as

$$g = \bar{g} m^a h^b, \tag{1.4}$$

where m is the probability of an activation gate being in the open state, h is the probability of an inactivation gate being in the open state, being 0 for closed and 1 for opened, a is the number of activation gates, b is the number of inactivation gates, being $a + b$ the total sum of gates, and $\bar{g}$ is the maximum conductance when all the channels are opened. The parameter $\bar{g}$ is determined experimentally and it is considered constant for each ion. If an inactivation gate is completely opened, the channel is blocked and ions cannot pass through. Probabilities m and h are also known by gating variables and are not constant due to the procedure of creating an action potential, as we are going to see in section 1.4.

1.3 Equations of the Hodgkin-Huxley model

Combining equations (1.1), (1.3) and (1.4) and assuming that in the squid giant axon there are three major current: the potassium current, with 4 activation gates with probability n each and 0 inactivation gates, the sodium current, with 3 activation gates with probability m each and 1 inactivation gate with probability h, and the leaky current(carried out mostly by chlorine ions) with no activation gates, i.e. with $a = b = 0$ in equation (1.4) and $g_L = \bar{g}_L$, we can express the Hodgkin-Huxley gate model

$$C_m \dot{V} = I_{ext} - \bar{g}_K n^4 (V - E_K) - \bar{g}_{Na} m^3 h (V - E_{Na}) - g_L (V - E_L), \tag{1.5}$$

where I_{ext} is the applied current and each activation variable changes with respect to time so we have

$$\begin{aligned}
\dot{n} &= \alpha_n(V)(1-n) - \beta_n(V)n = \left(\frac{\alpha_n(V)}{\alpha_n(V)+\beta_n(V)} - n\right)(\alpha_n(V)+\beta_n(V)),\\
\dot{m} &= \alpha_m(V)(1-m) - \beta_m(V)m = \left(\frac{\alpha_m(V)}{\alpha_m(V)+\beta_m(V)} - n\right)(\alpha_m(V)+\beta_m(V)),\\
\dot{h} &= \alpha_h(V)(1-h) - \beta(V)h = \left(\frac{\alpha_h(V)}{\alpha_h(V)+\beta_h(V)} - n\right)(\alpha_h(V)+\beta_h(V)),
\end{aligned} \tag{1.6}$$

where

$$\begin{aligned}
\alpha_n(V) &= 0.01\frac{10-V}{\exp\left(\frac{10-V}{10}\right)-1}, & \beta_n(V) &= 0.125\exp\left(\frac{-V}{80}\right),\\
\alpha_m(V) &= 0.1\frac{25-V}{\exp\left(\frac{25-V}{10}\right)-1}, & \beta_m(V) &= 4\exp\left(\frac{-V}{18}\right),\\
\alpha_h(V) &= 0.07\exp\left(\frac{-V}{20}\right), & \beta_h(V) &= \frac{1}{\exp\left(\frac{30-V}{10}\right)+1},
\end{aligned} \tag{1.7}$$

creating a coupled four-dimensional system.

The Nernst equilibrium potentials and the maximal conductance are predetermined at a temperature of $6.3C^{\circ}$, see [4], as

$$\begin{aligned}
E_k &= -12mV, & E_{Na} &= 120mV, & E_L &= 10.6mV,\\
\bar{g}_K &= 36mS/cm^2, & \bar{g}_{Na} &= 120mS/cm^2, & g_L &= 0.3mS/cm^2.
\end{aligned} \tag{1.8}$$

The membrane conductance, C_m, is considered 1 in all experimental data Hodgkin-Huxley used. Functions $\alpha_x(V)$ and $\beta_x(V)$ for $x = n, m, h$ describe the transition rates between open and closed states of the channels and are voltage-depending functions. These two functions are wisely chosen experimentally to match experimental data using the voltage-clamp technique.

Definition 1.6. *Steady-state activation or inactivation value(n_∞, m_∞ and h_∞) is a value that the gating variables tend to when time tens to infinite and the membrane voltage is clamped. The steady-state value is given by the expression*

$$x_\infty = \frac{\alpha_x}{\beta_x + \alpha_x}, \tag{1.9}$$

for $x = n, m, h$.

Commonly the model is used in a standard form applying the forward change of variables: $x_\infty = \frac{\alpha_x}{\alpha_x+\beta_x}$ and $\tau_x = \frac{1}{\alpha_x+\beta_x}$ for $x = n, m, h$, being x_∞ the steady-state activation or inactivation function and τ_x the voltage-dependent time constants. Hence, we can rewrite (1.6) as

$$\dot{n} = \frac{n_\infty(V) - n}{\tau_n(V)}, \qquad \dot{m} = \frac{m_\infty(V) - m}{\tau_m(V)}, \qquad \dot{h} = \frac{h_\infty(V) - h}{\tau_h(V)}.$$

The former equations can be solved as $x(t) = x_\infty + (x_o - x_\infty)\exp\left(\frac{t}{\tau_m}\right)$ defining the initial value as $x(0) = x_0$ for $x = n, m, h$.

Hodgkin-Huxley model is a one-parametric four-dimensional model having only the applied current, I_{ext}, as a parameter. Hence, if we want to study its dynamics, we have to study the different kinds of bifurcations being I_{ext} the bifurcation parameter. Nevertheless, there is a huge limitation when computing the bifurcation diagram of the model because of its dimension. In consequence, there have been studies on simpler planar vector fields and other simpler systems that illustrate some of the solutions of the model, but of course not that exhaustive. For example, we find a twisted homoclinic orbit that for topological reasons cannot be found in a planar system, but there are planar systems that have the same qualitative properties as the Hodgkin-Huxley without its complexity and having an easier analysis. Some of this simpler models are going to be discussed in sections 1.6 and 2.1.1 and in chapter 2.

1.4 Action potential on Hodgkin-Huxley model

Figure 1.2 shows how an action potential, an abrupt change in membrane voltage, works being $V_{rest} = 0$ the resting state [7]. Due to the higher extracellular concentration of Na^+, the current of Na^+ flows in, i.e. the probability function $m(t)$ is no longer zero and it starts to increase. This inflow leads to an upstroke on the membrane voltage until the sodium Nernst equilibrium is reached, as we can see on the blue point in figure 1.2. In consequence and in order to stabilize the membrane voltage, the activation of Na^+ current leads to a decrease in $h(t)$ and to an increase in $n(t)$ augmenting the K^+ outward current. When all activation and inactivation gates are active, the membrane voltage repolarizes again decreasing the membrane voltage until reaching the potassium Nernst equilibrium, the

[7] The resting state is considered $V_{rest} = -70mV$ in most of the references and experiments, but sometimes is normalized to be at zero, as in [2].

orange point on figure 1.2, and going through a period where the neuron is not capable of spiking again, called refractory period.

Definition 1.7. *A refractory period is a period where there is no possibility of a new action potential and it is located after the upstroke and right before the resting state.*

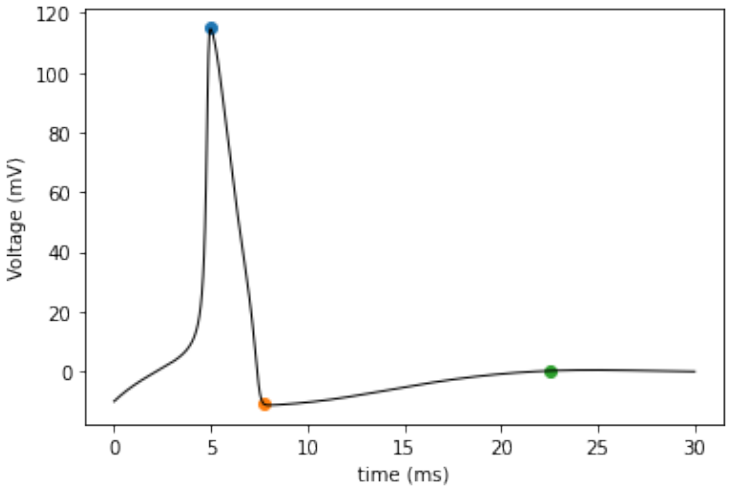

Figure 1.2: Action potential in Hodgkin-Huxley model when $I_{ext} = 0$. Figure obtained using the code A.1 with parameters as (1.8) and equations (1.5) and (1.6).

There is no possibility of a new spike until the neuron is on its recovery phase, close to the resting state and when $n(t)$ and $h(t)$ stabilize. When the membrane voltage is close to V_{rest}, recovery of $n(t)$ and $h(t)$ is slow, as we can see in figure 1.3, where we displayed the gating variables functions. Hence, the outward K^+ current is still activated causing V to go below V_{rest} causing what is called an after-hyperpolarization, depicted on figure 1.2 between the orange and the green point. We can see how the resting state is a stable equilibrium, even if we have a strong or a brief depolarization and even if there is inward current enough to generate a spike, the neuron goes back to rest.

On figure 1.3, we can prove that all functions stabilize and tend to a number, which has to be the steady-state value. Using the equation (1.9) and the code in A.1, we can calculate the steady-state value and see if it concurs with figure 1.3. For the potassium activation function, $n(t)$, probability functions stabilize to $\alpha_n \approx 0.05820$ and $\beta_n \approx 0.12499$, being $n_\infty \approx 0.31768$, concurring with the red curve in figure 1.3. For the sodium activation function, $m(t)$, probability functions stabilize to $\alpha_m \approx 0.22357$ and $\beta_m \approx 3.99994$, being $m_\infty \approx 0.05293$, concurring with the red curve on figure 1.3. Finally, for the sodium inactivation function, $h(t)$, proba-

bility functions stabilize to $\alpha_h \approx 0.069999$ and $\beta_h \approx 0.04743$, being $h_\infty \approx 0.59811$, concurring with the approximate 0.6 value that the black curve tends to in figure 1.3. In addition, we can also see that $m(t)$ initializes and stabilizes fast, faster than the others, and also reaches the maximum value. Activation variable $m(t)$ is incredibly fast, leading to simpler models not taking into account this gating variable, such as Morris-Lecar model discussed on section 1.6. Furthermore, we can also see that when $m(t)$ starts to increase, $h(t)$ starts to decrease and $n(t)$ starts to increase, according to the process of creating an action potential explained before.

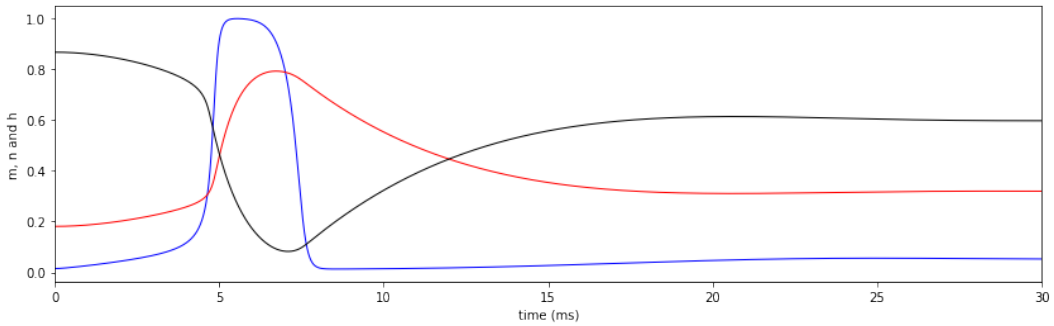

Figure 1.3: Gating variable functions in Hodgkin-Huxley model when $I_{ext} = 0$, being the sodium activation function, $m(t)$, the blue curve, the potassium activation function, $n(t)$, the red curve and the potassium inactivation function, $h(t)$, the black curve. Figure obtained using the code A.1 with parameters as (1.8) and equations (1.5) and (1.6).

In both figures, we have seen that the fast activation and the slow inactivation of the sodium current is the reason for the creation of an action potential. Hence, the amplitude of the action potential depends on the concentration of sodium on the outside of the cell.

1.5 Analysis of the model

When the injected current is low, the cell remains quiescent; when the injected current is higher, the cell can fire repetitively or a single spike depending on the intensity of the current injected. If the current we apply is bigger and longer enough we can have a periodic spiking.

Definition 1.8. *A periodic spiking is a set of action potentials that happen repeatedly not necessarily with the same amplitude each. In this case, we have a transition from quiescent to repetitive spikes. From the dynamical systems point of view, we have a transition from a stable equilibrium point to a stable limit cycle considering the injected current, I_{ext}, our bifurcation parameter.*

I computed a voltage over time graph that exhibits the behaviour of the action potentials for different values of I_{ext}, for different values of applied current. In addition, I graphed how the activation and inactivation gating variables behave for different values of applied current. I computed it using Colab and Python language and using the experimental data Hodgkin and Huxley used, considering $C_m = 1pF/cm^2$, a temperature of $6.3C^\circ$ and all the constant parameters as in (1.8). When defining the intracellular potential, one is free to choose a convention that defines the resting intracellular potential or the extracellular potential to be zero. I assumed that my initial potential in this study is $V = -70mV$, so my extracellular potential is 0 and my intracellular potential would be $70mV$ at first.

When I apply a current that is constantly 0, $I_{ext} = 0\mu A$, only one spike is generated and then it goes directly to rest, without any kind of oscillation exhibiting the same structure as figure 1.2 and 1.3. In consequence, the V_{rest} is a stable equilibrium point.

If we apply a constant intensity of $20\mu A$, $I_{ext} = 20\mu A$, a periodic spiking activity is observed in figure 1.4. A stable limit cycle was born and the amplitude of it is constant except from the first spike. If we do not apply any change, the neuron would spike forever via a periodic spiking behaviour.

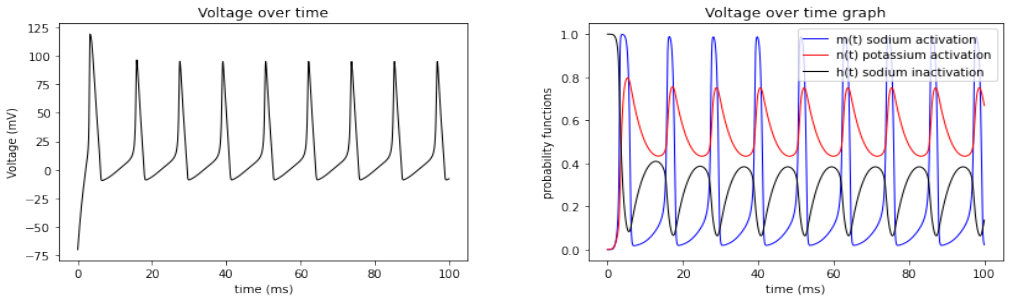

Figure 1.4: Action potential(left) and activation and inactivation of sodium and potassium channels(right) on Hodgkin-Huxley model when $I_{ext} = 20\mu A$. Figure obtained using the code A.1 with $C_m = 1$, $T = 6.3C^\circ$, parameters as in (1.8) and equations (1.5) and (1.6).

When we keep augmenting the intensity, the periodicity of the spikes is being maintained but its amplitude is lower every time until a certain value is reached and the neuron does not spike and goes back to rest. In figure 1.5, where we applied an intensity current of $75\mu A$, the amplitude of the action potential is lower and it would be even lower if we keep on increasing the applied current.

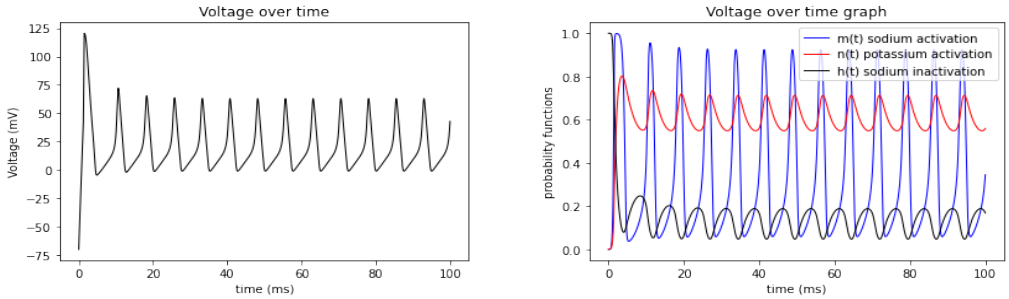

Figure 1.5: Action potential(left) and activation and inactivation of sodium and potassium channels(right) on Hodgkin-Huxley model when $I_{ext} = 75\mu A$. Figure obtained using the code in A.1 with $C_m = 1$, $T = 6.3°$, parameters as in (1.8) and equations (1.5) and (1.6).

Provided that a certain value of I_{ext} is reached, approximately around $I_{ext} = 125\mu A$, the neuron is not able to spike periodically and it goes back to rest oscillating, as we can see in figure 1.6. In this case, V_{rest} is a stable equilibrium point and the stable limit cycle has vanished. We can see that our equilibrium point is approximately $V = 25mV$. In fact, if we solve the equation (1.5) for V, being $I_{ext} = 200$, $C_m = 1$, g_x and E_x for $x = Na, K, L$ as (1.8) and the activation and inactivation function being equal to their steady-state value for this applied intensity, i.e. $n(t) = n_\infty = 0.669956$, $m(t) = m_\infty = 0.479992$ and $h(t) = h_\infty = 0.054814$, we get the solution $V \approx 24.5702$, concurring with figure 1.6(left).

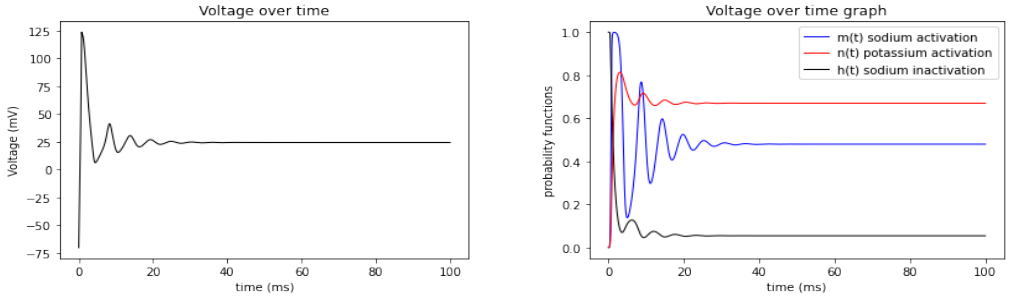

Figure 1.6: Action potential(left) and activation and inactivation of sodium and potassium channels(right) on Hodgkin-Huxley model when $I_{ext} = 200\mu A$. Figure obtained using the code in A.1 with $C_m = 1$, $T = 6.3C°$, parameters as in (1.8) and equations (1.5) and (1.6).

If we keep on augmenting the applied current over $I_{ext} = 200\mu A$, the oscillations before going back to rest are shorter every time. If we keep on augmenting the intensity, the action potential resembles the one in figure 1.2.

We can also study the phase plain of the activation and inactivation variables over other activation and inactivation variables and over voltage. For example, we can plot the (n, h), (m, n) and (V, n) graph when $I_{ext} = 15\mu A$, following [10].

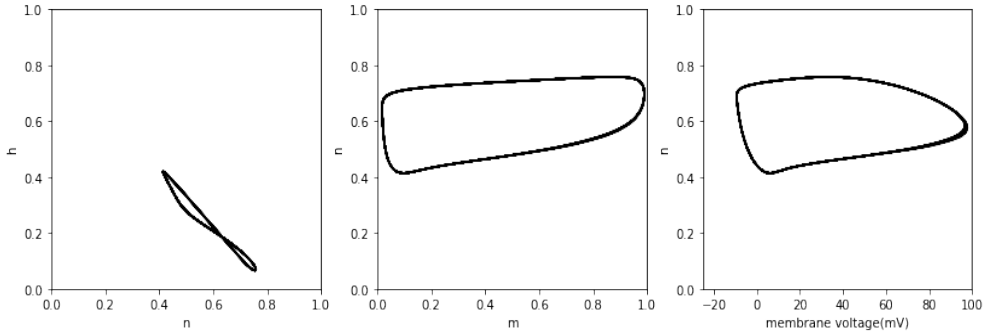

Figure 1.7: Phase plane projections for equations (1.5) and (1.7). The left one is n versus h, the center one is m versus n and the left one is V versus n. Figures obtained from A.1 with $I_{ext} = 15\mu A$, $C_m = 1$, the values of the parameters as in (1.8) and the equations (1.5) and (1.6).

In figure 1.7(left), we can see that there exists a correlation between the activation variable of the potassium, n, and the inactivation of the sodium, h, concretely $h \approx 0.8 - n$, see [4]. In addition, in figure 1.7(center), we can see how the activation variable of the sodium, m, is faster than the activation variable of the potassium, n, concurring with the procedure of creating an action potential explained in section 1.4 and with figure 1.3. Lastly, in figure 1.7(right) we can see how the value of n oscillates creating a limit cycle over the membrane voltage, V.

To sum up, the (t, V)-graph passes through three stages: an equilibrium stage, a single-spike stage and a limit cycle stage, i.e. periodic spiking stage. When no external current is applied, we have a stable equilibrium point. If the external input increases enough, a stable limit cycle is created undergoing a supercritical Andronov Hopf bifurcation, the bifurcation associated with the birth of a limit cycle from a stable equilibrium point. Moreover, if we increase the external applied current the system has a stable equilibrium point again undergoing an Andronov Hopf bifurcation, explained in section 2.3.1.

1.6 Morris-Lecar model

Hodgkin-Huxley model is capable of exhibiting a single spike, a train of spikes, periodic spikes, bursting and chaotic behaviour.

Definition 1.9. *Bursting is a neuron behaviour created when there is a period of spiking activity followed by a period of quiescent activity and creating a periodic loop of quiescent and spiking activity.*

Simplifying Hodgkin and Huxley model can lead to new models that can not exhibit complex and important behaviour as bursting and chaos. Via bursting behaviour, neurons are capable of transmitting a wide range of information, less information is transmitted on a single spike. Hence, Morris-Lecar model should be considered as it is a simpler model that can be used in other systems that exhibit bursting behaviour.

Catherine Morris and Harold Lecar[17] started studying the barnacle muscle fiber, which has an added calcium current and started working on a reduced system of Hodgkin-Huxley model based on the relevant fact that the sodium current can be considered instantaneous, as we can see in figure 1.3, being Ca^+ and K^+ the only currents considered, besides the leakage current that is also considered. In consequence, it is also known as $I_{Ca} + I_k$ model. This model exhibits similar topology results as Hodgkin-Huxley model but it is a two-dimensional model and, in consequence, easier to analyze.

Morris-Lecar model combines the simplicity of FitzHugh-Nagumo model, which will be explained in chapter 2, with the biological details of Hodgkin-Huxley model. It is a multi-parameter model that with proper measurement of the parameters it can display a single spike or a train of spikes.

1.6.1 Equations of Morris-Lecar Model

We consider equation (1.5), delete the sodium current, add the calcium one, assume that the calcium has one activation gate with probability m, which is equal to the steady-state function, i.e. $m = m_\infty$, and we assume that the new variable, w, illustrates the variation over time of the probability function of the activation gate of the potassium, n, and of the inactivation gate of the calcium, h. According to the previous, we arrive at the following Morris-Lecar equations

$$\begin{aligned} C_m\dot{V} &= I_{ext} - g_{Ca}m_\infty(V)(V - E_{Ca}) - g_K w(V - E_K) - g_L(V - E_L), \\ \dot{w} &= \lambda(V)(w_\infty(V) - w), \end{aligned} \tag{1.10}$$

where C_m is the membrane capacitance, g_k is the respective constant conductance for $k = Ca, K, L$, w is the recovery variable of the voltage membrane and E_k are the respective Nernst equilibrium potentials for $k = Ca, K, L$. There are two persistent voltage-gated currents: the depolarizing current is carried by Ca^{2+} and the hyperpolarizing current by K^+.

The steady-state values are defined as:

$$\begin{aligned} m_\infty(V) &= \frac{1}{2}\left(1 + \tanh\left(\frac{V - V_1}{V_2}\right)\right), \\ w_\infty(V) &= \frac{1}{2}\left(1 + \tanh\left(\frac{V - V_3}{V_4}\right)\right), \\ \lambda(V) &= \frac{1}{3}\cosh\left(\frac{V - V_3}{2V_4}\right), \end{aligned} \tag{1.11}$$

where V_1, V_2, V_3 and V_4 are voltage parameters that are adjusted to have the wished pattern. This model is considered the fast subsystem in a lot of fast-slow systems and, most important, a lot of fast-slow bursters, systems that exhibit bursting, i.e. using the equation (1.10) and a linear slow subsystem, we can create a system that exhibits bursting behaviour, as we are going to see in chapter 3.

1.7 Excitability

We are going to define what is known as an excitable neuron and how Hodgkin and Huxley classified neurons via their excitability.

Definition 1.10. *The threshold is the place where the decision to fire or not to fire is made. If the membrane voltage is below the threshold, the neuron does not exhibit an action potential or a spike.*

Definition 1.11. *A neuron is quiescent if the membrane potential is at rest or it illustrates small amplitude oscillations, called subthreshold oscillations.*

Definition 1.12. *Subthreshold oscillations are small amplitude oscillations located on the resting state being consequence of stable equilibrium points or small stable limit cycles on the resting state. These kinds of oscillations are not significant enough to be considered action potentials.*

Definition 1.13. *A neuron is excitable when a small perturbation on the quiescent state due to input currents results in a long orbit before it comes back to quiescent, which corresponds to a fixed point. Such a long orbit is what we call an action potential or spike.*

When the former orbit is a large amplitude limit cycle, the neuron can fire periodically creating a sequence of spikes.

From the dynamical systems point of view, a neuron is excitable because it is near a bifurcation for a change on I_{ext}, i.e. a transition from quiescence to repetitive firing or backward varying the bifurcation parameter I_{ext}. If we have a system that has a global attractor equilibrium point(for example a stable focus), it is excitable if there is a large amplitude periodic pseudo-orbit passing near the equilibrium. Otherwise, small perturbations will not create longer trajectories that lead to action potentials, being impossible for a neuron to spike.

Definition 1.14. *Being $I \subseteq \mathbb{R}$ an interval of time, $t_0, t_1 \in I$ the initial and the final instant respectively and $x(t)$ the solution of the equation at the instant t, if $\|x(t_1) - x(t_0)\| < \epsilon$, being ϵ small enough, the orbit is called a periodic ϵ-pseudo-orbit.*

There is a famous classification of neurons in integrators or resonators. Moreover, Hodgkin and Huxley also suggested a way of classifying neurons.

Definition 1.15. *A neuron acts as an integrator if an increase in the frequency of the incoming current leads to a spike sooner. The more frequency we apply, the sooner the spike is generated. These kinds of cells have the property of all-or-none spikes*[8] *with a low frequency.*

Definition 1.16. *A neuron acts as a resonator if it only responds to a certain frequency input. These kinds of neurons do not have the all-or-none spike property and a well-defined threshold.*

1.7.1 Classification of excitability according to Hodgkin and Huxley

Hodgkin and Huxley proposed a classification via the class of excitability of the neuron determined by the frequency of the emerging spike, i.e. the frequency of the large amplitude limit cycle that appears.

Class 1 neural excitability

Action potentials can be generated with a low frequency and the frequency increases if we increase the applied current. This kind of neuron can exhibit oscillations with a low frequency and the interval between every oscillation is random since this kind of neuron is sensitive to small perturbations of time. Class 1 excitable neurons are considered integrators.

[8] All-or-none spikes happen when either the solution crosses the threshold producing a spike or the solution orbit does not cross the threshold and it goes directly back to rest.

Class 2 neural excitability

Action potentials are generated in a certain frequency interval, which is insensitive to changes in the applied current and varies from neuron to neuron. These kinds of neurons are quiescent or firing with a regular interspike[9]. Unlike class 1 neurons, they can fire in response to weak inhibitory pulse, known as post-inhibitory spikes. After the spike, they have a period where they can exhibit another spike without applying any added current. Neurons that exhibit class 2 neural excitability are resonators.

There is a last and less used classification of neurons called Class 3 neural excitability, which corresponds to a single action potential in response to a pulse of current. Its inability to generate a sequence of spikes makes it simpler and less relevant.

[9]Interspike is the period between every spike or every action potential.

Chapter 2

FitzHugh-Nagumo Model

The Hodgkin-Huxley model is considered a model that exhibits the major phenomena that are observed in neuron activity: resting or quiescence, action potential or spiking, chaotic behaviour and bursting. Due to its dimension, they focused on studying simpler models that allowed to compute effective phase planes.

2.1 Background of the equations: Van der Pol oscillator.

The equations of the FitzHugh-Nagumo model are based on the Van der Pol equation, they studied the Van der Pol oscillator and modified it in order to get periodical spiking behaviour.

Definition 2.1. *[12] The Van der Pol equation is a differential equation that exhibits the temporal evolution of a non-conservative* [1] *oscillator with nonlinear damping*[2] [3]*. The basic system can be written in the form*

$$\ddot{x} + \mu\phi(x)\dot{x} + x = \beta p(t),$$

where $\dot{x}$ is the derivative with respect to time, i.e. $\dot{x} = \frac{dx}{dt}$, $\phi(x)$ is an even function and $\phi(x) < 0$ for $|x| < 1$ and $\phi(x) > 0$ for $|x| > 1$. The function $p(t)$ is a periodic function that in most neuronal models is considered zero, and μ and β are non-negative parameters.

When $\beta = 1$ and $\phi(x) = x^2 - 1$, the differential equation that describes the movement of such oscillator is

$$\ddot{x} + \mu(x^2 - 1)\dot{x} + x = p(t), \tag{2.1}$$

[1] A non-conservative force is a force where the total work done is independent of the path taken.

[2] Damping is the process that dissipates the energy stored in an oscillation. It is an influence that affects reducing or preventing the oscillation.

[3] Nonlinear damping occurs when the energy is dissipated at large amplitudes and generated at low amplitudes.

where x is a function of time, t, that indicates the position and $\mu \in \mathbb{R}$ indicates the nonlinearity and the strength of the damping. When $\mu = 0$, the equation describes the simple harmonic oscillator with non-damping and with conservation of energy. When $\mu > 0$, the system enters a stable limit circle near the origin. Near the origin the system is stable and far from it is damped. Moreover, if x is small, x^2 is negligible creating a system with negative damping and, if x is large, the system has positive damping due to the dominance of the quadratic term. Concerning equation (2.1) phase plain, we can state that the nullclines are a vertical and a cubic line that intersect in a single equilibrium point, $(x, y) = (0, 0)$, and its stability depends on μ, as we are going to see in section 2.1.1.

Being $p(t) = 0$ and renaming $g(x) = x$ and $f(x) = \mu(x^2 - 1)$ in equation (2.1), we have a Liénard equation.

Definition 2.2. *[18] Let f and g be two continuous and differential functions on $\mathbb{R}$, being f an even and g an odd function. The second order differential equation of the form*

$$\ddot{x} + f(x)\dot{x} + g(x) = 0 \tag{2.2}$$

is called a Liénar equation.

We can rewrite Liénard equation (2.2), using a change of variable $x = x$ and $y = \dot{x}$, getting a two-dimensional system

$$\dot{x} = y, \qquad \dot{y} = -f(x)y - g(x), \tag{2.3}$$

and using the Liénard transformation $\bar{y} = y + F(x)$, being $F(x) = \int_0^x f(\xi)d\xi$, and renaming $y = \bar{y}$, the previous system can be rewritten in the form

$$\dot{x} = y - F(x), \qquad \dot{y} = -g(x).$$

Considering $F(x) = \mu\Phi(x)$, where $\Phi(x) = \int_0^x \phi(\xi)d\xi$ and $\phi(x)$ is the even function quoted in definition 2.1, and applying the change $\hat{y} = y/\mu$, we get

$$\dot{x} = \mu(y - \Phi(x)), \qquad \dot{y} = \frac{-g(x)}{\mu},$$

and applying the change on time $\tau = -\mu t$ we get a system that starts to resemble the equations of the FitzHugh-Nagumo model, equations (2.10),

$$\begin{aligned} \dot{x} &= \Phi(x) - y, \\ \dot{y} &= \frac{1}{\mu^2} g(x), \end{aligned} \tag{2.4}$$

assuming $\mu \neq 0$.

The main reason why they used the Van der Pol equation is that the Van der Pol equation satisfies the Liénard theorem.

Theorem 2.3. *Liénard Theorem[18][25]: If a Liénard equation, i.e. the equation* (2.2)*, satisfies the following conditions:*

1. $f : \mathbb{R} \to \mathbb{R}$ *and* $g : \mathbb{R} \to \mathbb{R}$ *are continuous;*
2. $F(x) = \int_0^x f(\xi)d\xi$ *is an odd function in* x*, i.e.* $F(-u) = -F(u)$*;*
3. $\lim_{x\to+\infty} F(x) = \infty$*;*
4. *Exists* $u > 0$ *such that* $F(x) < 0$ *if* $0 < x < u$*;*

then the system has a unique and attractor limit cycle surrounding the origin.

The existence of the stable limit cycle leads to the existence of periodic spiking and action potentials, making Van der Pol equations more appealing for neuroscientists.

2.1.1 Forced Van der Pol oscillator

The Van der Pol oscillator does not present chaotic behaviour, but using a sinusoidal force, i.e. being $p(t)$ in equation (2.1) a sinus function, it might exhibit periodic oscillations leading to chaos and bursting behaviour, as we are going to see below. Hence, modifying the forced Van der Pol oscillator can lead to systems that can exhibit bursting behaviour.

Definition 2.4. *The forced Van der Pol oscillator follows the differential equation*

$$\ddot{x} - \mu(1 - x^2)\dot{x} + x - A\sin(\omega t) = 0, \tag{2.5}$$

where $x(t)$ *is the position function over* t*,* $\mu \in \mathbb{R}$ *indicates the nonlinearity and the strength of the damping,* A *is the amplitude or displacement of the oscillator from the equilibrium point and* ω *is the angular velocity.*

We can rewrite equation (2.5) using the change of variables $x = x$ and $\dot{x} = y$ as

$$\begin{aligned} \dot{x} &= y, \\ \dot{y} &= \mu(1 - x^2)y - x + A\sin(\omega t), \end{aligned} \tag{2.6}$$

having a non-autonomous system, a system that depends on the time. Hence, if we consider $A = 0$, we have an autonomous system without any periodic force

that has a unique equilibrium point at $(0,0)$ that its stability depends on μ. In consequence, if $\mu > 2$, it is an unstable node; if $0 < \mu < 2$, it is an unstable focus; if $\mu = 0$, we have the harmonic oscillator and it is a center; if $-2 < \mu < 0$, it is a stable focus; if $\mu < -2$, it is a stable node.

When $A \neq 0$, we do not have that equilibrium point because it changes over time. We are going to see via the implicit function theorem and the Poincaré map that such equilibrium point evolves creating a $2\pi/\omega$-periodic orbit.

Theorem 2.5. *(Implicit function theorem): Let*

$$\begin{array}{rccc} f\colon & I \times \Lambda \subset \mathbb{R}^n \times \mathbb{R}^m & \longrightarrow & \mathbb{R}^m \\ & (x,\lambda) & \longmapsto & f(x,\lambda) \end{array}$$

be a continuously differentiable function and with parameter $\lambda \in \mathbb{R}^m$, and $(x_0,\lambda_0) \in \mathbb{R}^n \times \mathbb{R}^m$ a fixed point, i.e. $f(x_0,\lambda_0) = 0 \in \mathbb{R}^m$. If the determinant of $D_x f(x_0,\lambda_0)$ is different from zero, i.e. $det(D_x f(x_0,\lambda_0)) \neq 0$, there exists $I_0 \times \Lambda_0 \subset I \times \Lambda$, a neighbourhood of (x_0,λ_0), and a continuously differentiable function $\bar{x} : \Lambda_0 \longrightarrow I_0$ such that $f(\bar{x}(\lambda),\lambda) = 0$ for all $\lambda \in \Lambda_0$.

Definition 2.6. *Let Ω be the phase space and $\varphi(t;x_0,y_0,A)$ the evolution process associated to a system in $\mathbb{R}^n$ with initial conditions (x_0,y_0) and with parameter A, the time-τ Poincaré(stroboscopic) map is*

$$\begin{array}{rccc} f\colon & \Omega \subset \mathbb{R}^n \times \mathbb{R} & \longrightarrow & \mathbb{R}^n \\ & (x_0,y_0,A) & \longmapsto & P(x_0,y_0,A) = \varphi(\tau;x_0,y_0,A) \end{array}$$

If we want to see that the equilibrium point (x,y) for a parameter value A of the autonomous system is a $2\pi/\omega$-periodic orbit at the non-autonomous, we have to see that is a fixed point of the Poincaré map, i.e. $P(2\pi/\omega;x,y,A) = (x,y,A)$, having an orbit of period τ. Hence, we are going to apply the implicit function theorem to the map $g(x,y,A) = P(2\pi/\omega;x,y,A) - (x,y,A)$, being $(x,y) = (0,0)$ and $A = 0$, since it is the only equilibrium point when $A = 0$.

Let's see if the conditions of the theorem 2.5 hold. First, applying that $(0,0)$ is a fixed point when $A = 0$, $g(0,0,0) = P(2\pi/\omega;0,0,0) - (0,0,0) = (0,0)$. Secondly, we need $det(D_{(x,y)}g(0,0,0)) \neq 0$. Taking into account the definition of the function g, we have $det(D_{(x,y)}g(0,0,0)) = det(D_{(x,y)}\varphi(2\pi/\omega,0,0) - Id)$. Solving the first variational and evaluating on $t = 2\pi/\omega$, we get

$$det(D_{(x,y)}\varphi(2\pi/\omega,0,0) - Id) = \left(-1 + \exp\left((\mu - S)\,\pi/\omega\right)\right)\left(-1 + \exp\left((\mu + S)\,\pi/\omega\right)\right),$$

where $S = \sqrt{\mu^2 - 4}$.

When $\mu \neq 0$, the determinant does not vanish. When $\mu = 0$ and the frequency is $2\pi k/\omega$ for $k \in \mathbb{Z}$, the determinant is 0. Hence, we can apply the implicit function theorem when $\mu \neq 0$ and we have proved the existence of a periodic orbit of period $2\pi/\omega$.

As we have stated, the forced Van der Pol oscillator might present chaotic behaviour. In consequence, we are going to illustrate such chaotic behaviour with parameters $A = 1.05$, $\mu = 7.48$ and $\omega = 2\pi/10$ in system (2.6). Integrating the system and representing in a $\dot{x} - x$ graph every $2\pi/\omega$ seconds, we get the phase plane with a possible strange attractor independent from the initial conditions we consider.

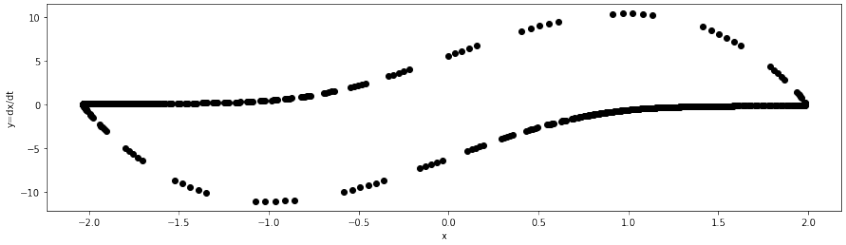

Figure 2.1: Possible chaotic behaviour in system (2.6) with parameter values $(A, \omega, \mu) = (1.05, 2\pi/10, 7.48)$, values taken from [29] and figure obtained via the code in A.2.

In figure 2.1, we have plotted 1000 iterates of the Poincaré map with initial condition $(0, 0)$ and we can see what resembles a strange attractor because the iterates do not fill the whole attractor limit cycle. If we restrict to such attractor, we have sensibility over initial conditions leading to a possible chaotic behaviour, see [29] for further details.

2.2 Equations of the model

FitzHugh and Nagumo aimed to find a two-dimensional model that imparted a mathematical idea about the mechanism of neuron excitability. A model that imitated qualitatively the generation of an action potential, as Hodgkin-Huxley model did, without taking into account ionic currents.

Definition 2.7. *A fast-slow system is a $\mathbb{R}^n$ system*

$$\dot{x} = f(x, y), \tag{2.7}$$

$$\dot{y} = \epsilon g(x, y), \tag{2.8}$$

where $x \in \mathbb{R}^m$, $y \in \mathbb{R}^{n-m}$, f and g are two continuous functions and $\epsilon \in \mathbb{R}$, $0 < \epsilon \ll 1$ the parameter that creates a slow dynamic for the variable y. The equation (2.7) *is considered the fast subsystem and* (2.8) *is considered the slow one.*

Remark 2.8. As a fast-slow system has two time-scales, we can study the fast subsystem applying the change of variable $\tau = \epsilon t$ in (2.7) and (2.8), getting

$$\begin{aligned} \dot{x} &= \frac{1}{\epsilon} f(x, y), \\ \dot{y} &= g(x, y), \end{aligned}$$

being $\epsilon \approx 0$ a positive parameter.

FitzHugh and Nagumo wanted a two-dimensional fast-slow system

$$\begin{aligned} \dot{V} &= f(V, w), \\ \dot{w} &= \epsilon g(V, w), \end{aligned} \tag{2.9}$$

where V is the membrane voltage, w is a recovery value of the membrane voltage that mimics activation of an outward current, needed because the neuron activates during an impulse and then goes back to the initial resting, and ϵ is a constant that bestows the slow-fast dynamic wanted and it controls the speed of the slow variable, as we have seen in definition 2.7. Hence, the recovery value is considered to evolve in much slower time-scaling than the membrane voltage.

FitzHugh and Nagumo studied the fast-slow systems and modified the Van Der Pol equation (2.2) getting

$$\begin{aligned} \dot{V} &= \Phi(V) - w + I_{ext}(t), \\ \dot{w} &= \epsilon(g(V) - vw), \end{aligned} \tag{2.10}$$

where $\Phi(V)$ is a cubic function that forms oscillations, $g(V)$ is a linear monotonically increasing function, v is a constant parameter and $I_{ext}(t)$ is the injected current that is modified over time. We can observe that if $v = 0$ and $I_{ext}(t) = 0$, we have the system (2.4) being $\epsilon = 1/\mu^2$.

2.3 Analysis of the model

The model is commonly analyzed with the form

$$\begin{aligned} \dot{V} &= V - \frac{V^3}{3} - w + I_{ext}, \\ \dot{w} &= 0.08(V + 0.7 - 0.8w), \end{aligned} \tag{2.11}$$

assuming that $I_{ext}(t)$ is constant, i.e. $I_{ext}(t) = I_{ext}$ and $\Phi(V) = V - V^3/3$, $g(V) = V + 0.07$, $\epsilon = 0.08$ and $v = 0.8$ in system (2.10).

2.3.1 Andronov-Hopf bifurcation

The Andronov-Hopf bifurcation is associated with the appearance or disappearance of a limit cycle. In neuronal terms, having an Andronov-Hopf bifurcation leads to periodic spiking activity, so we are going to see if the FitzHugh-Nagumo model undergoes an Andronov-Hopf bifurcation.

In this kind of bifurcation, a periodic solution is born or destroyed at the equilibrium point, so no equilibrium points arise. When the limit cycle shrinks to the equilibrium point and disappears, the equilibrium point absorbs its stability. Meanwhile, if a limit cycle is born it absorbs the stability of the fixed point. Hence, there are two kinds of Andronov-Hopf bifurcations: supercritical and subcritical. The supercritical bifurcation occurs when the equilibrium at the bifurcation is stable. Whereas the subcritical one occurs when the bifurcation orbit is unstable.

Definition 2.9. *[28] Being*

$$\dot{x} = f(x, \alpha), x \in \mathbb{R}^n, \tag{2.12}$$

an autonomous system of ordinary differential equations and α our bifurcation parameter. If the system has a set of equilibrium points and the Jacobian matrix has one pair of complex eigenvalues

$$\lambda_{1,2}(\alpha) = \mu(\alpha) \pm i\omega(\alpha),$$

which becomes purely imaginary when $\alpha = 0$, i.e. $\mu(0) = 0$. If $\alpha = 0$, we have the purely imaginary eigen values $\lambda_{1,2} = \pm\omega_0$, being $\omega(0) = \omega_0$. Then, as α passes through $\alpha = 0$ we have an Andronov-Hopf bifurcation, the equilibrium point changes stability and a unique limit cycle bifurcates from it. Hence, the Andronov-Hopf bifurcation is characterized by a single bifurcation condition, $Re(\lambda_{1,2}) = 0$, being a codimensional one bifurcation.

Theorem 2.10. *(Andronov-Hopf Bifurcation Theorem)[28]: Let $\dot{f} = f_\alpha(x) = f(x, \alpha)$ be a family of systems of differential equations in $\mathbb{R}^n$ with equilibrium $\bar{x} = 0$ for all α. Let $\mu(\alpha) \pm i\omega(\alpha)$ denote a complex conjugate pair of eigenvalues of the matrix $Df_\alpha(0)$ that crosses the imaginary axis at a nonzero rate at $\alpha = 0$; that is, $\mu(0) = 0$, $\omega = \omega(0) \neq 0$, and $\mu'(0) \neq 0$. Then a path of periodic orbits bifurcates from $(\alpha, x) = (0, 0)$. The periods of these orbits approach $2\pi/\omega$ as orbits approach $(0, 0)$.*

On one hand, in figure 2.2, we plot the phase plain of the supercritical Andronov-Hopf bifurcation. Before the bifurcation, the equilibrium point is stable. During the bifurcation, a limit cycle is born absorbing the stability of the fixed points, i.e. an attractor limit cycle is born. After the bifurcation, the attractor limit cycle has expanded and the equilibrium point has lost its stability and now is unstable.

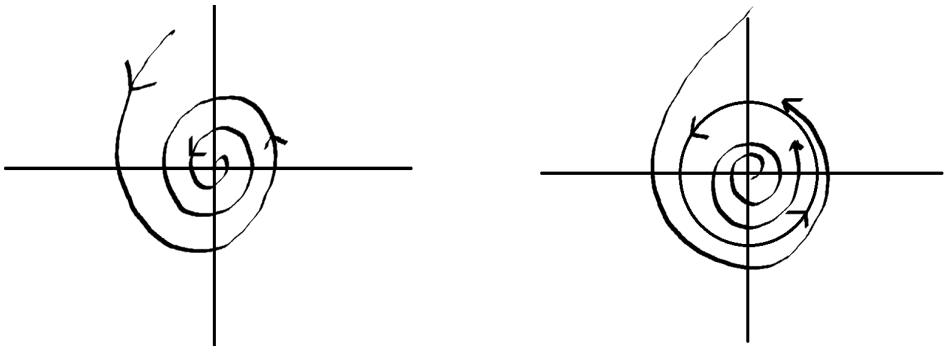

(a) Phase plain before the bifurcation. Parameter $\alpha < 0$ in the system (2.12).

(b) Phase plain after the bifurcation. Parameter $\alpha > 0$ in the system (2.12).

Figure 2.2: Phase plane of the system (2.12) modifying the bifurcation parameter α. When $\alpha = 0$, the supercritical Andronov-Hopf bifurcation occurs.

On the other hand, in figure 2.3, we illustrate the phase plain of the subcritical Andronov-Hopf bifurcation. Initially, we have a limit cycle surrounding the origin, which is unstable. During the bifurcation, the limit cycle shrinks onto the equilibrium point and the point absorbs the stability of the limit cycle. Hence, after the bifurcation, we have an unstable equilibrium point.

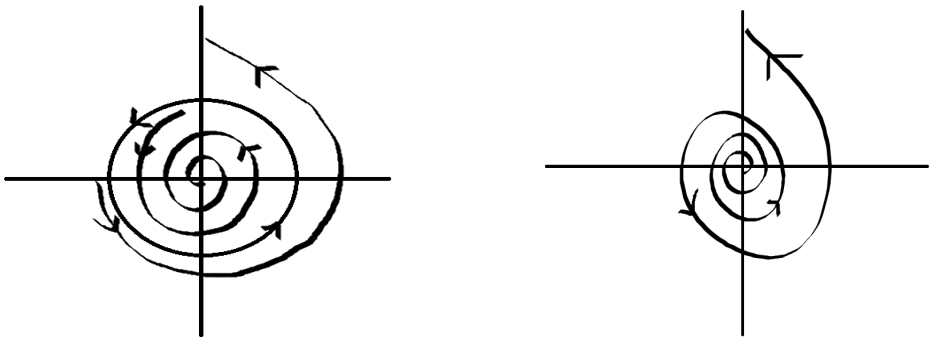

(a) Phase plain before the bifurcation. Parameter $\alpha < 0$ in the system (2.12).

(b) Phase plain after the bifurcation. Parameter $\alpha > 0$ in the system (2.12).

Figure 2.3: Phase plane of the system (2.12) modifying the bifurcation parameter α. When $\alpha = 0$, the subcritical Andronov-Hopf bifurcation occurs.

In the Andronov-Hopf bifurcation, we have a loss of stability because the eigenvalues go from having a real negative part to a real positive part, crossing the imaginary axis. Hence, if we want to study when there is an Andronov-Hopf bifurcation, the real part has to be equal to 0, having purely imaginary eigenvalues. Hence, the trace of the Jacobian matrix needs to be 0 and its determinant needs to be positive[4].

Once we have introduced the bifurcation, we are going to analyze if the system (2.11) undergoes an Andronov-Hopf bifurcation. Firstly, we are going to study the phase plain and we are going to compute the nullclines in order to find their intersections, i.e the equilibrium points,

$$w = V - \frac{V^3}{3} + I_{ext} \quad (V - nullcline),$$
$$w = \frac{V + 0.7}{0.8} \quad (w - nullcline),$$

getting the equilibrium points equation

$$\frac{-V^3}{3} - \frac{V}{4} - \frac{7}{8} + I_{ext} = 0. \tag{2.13}$$

In order to have an Andronov-Hopf bifurcation, we need one equilibrium point. Hence, we need the discriminant of the equation (2.13) to be negative[5], so we have $disc = -4(-\frac{1}{3})(-\frac{1}{4})^3 - 27(-\frac{1}{3})^2(-\frac{7}{8} + I)^2 = -3(I - \frac{7}{8})^2 - \frac{1}{48} < 0$.

We have seen that we only have one equilibrium point because the discriminant is always negative. Moreover, in order to have a Hopf bifurcation we need a purely imaginary eigenvalue, so the trace of the Jacobian matrix must be 0 and the determinant positive, as explained in section 2.3.1. Let X denote the vector field of equations (2.11), one has

$$DX(u, v) = \begin{pmatrix} -v^2 + 1 & -1 \\ 0.08 & -0.064 \end{pmatrix},$$

so the trace, τ, is $-V^2 + 0.936$ and the determinant, $\triangle$, is $0.064V^2 + 0.016$, which is always positive. In order to have the trace equal to 0, we need the solutions

[4]The eigenvalues, λ, of a matrix can be calculated solving the equations $\lambda^2 - \tau\lambda + \triangle$, where τ is the trace and $\triangle$ is the determinant of such matrix.

[5]Being $ax^3 + bx^2 + cx + d = 0$, $a \neq 0$, the discriminant of a cubic equations is defined as $disc = 18abcd - ab^3d + b^2c^2 - 4ac^3 - 27a^2d^2$. If $disc = 0$, the equations has multiple zeros. If $disc < 0$, the equation has one real and two conjugate complex solutions. If $disc > 0$ the equation has three different real solutions.

$V_1 \approx -0.967471$ and $V_2 \approx 0.967471$. For that value of membrane voltage, we have a Hopf bifurcation because the trace is 0 and the determinant is positive.

Solving the equilibrium equation (2.13), we get the value of the parameter, $I_{ext}(V)$, i.e. the value of the intensity current applied as $I_{ext}(V) = \frac{V^3}{3} + \frac{V}{4} + \frac{7}{8}$, so we get $I_{ext}^{(1)}(V_1) \approx 0.331281$ and $I_{ext}^{(2)}(V_2) \approx 1.41872$. We are going to study the bifurcations of each of the equilibrium points as a function of the parameter I_{ext}, being $(V_1, I_{ext}^{(1)}) \approx (-0.967471, 0.331281)$ and $(V_2, I_{ext}^{(2)}) \approx (0.967471, 1.41872)$ the equilibrium points, i.e. we are going to study if we have appearance or disappearance of a limit cycle.

According to figure 2.4(where I displayed the linear stability of the equilibrium points according to the determinant and the trace of the Jacobian matrix), if $\tau^2 - 4\triangle < 0$ and $\tau > 0$, we have an unstable focus. Nevertheless, if $\tau < 0$ we have a stable focus. In consequence, if $v \in (-0.967471, 0.967471)$, we have an unstable focus and if $v \notin (-0.967471, 0.967471)$ we have a stable focus.

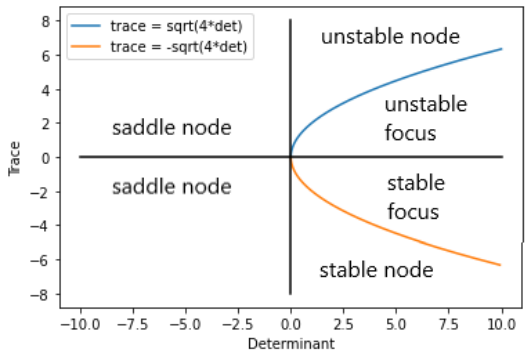

Figure 2.4: Classification of lineal stability of equilibrium points. Unstable focus: complex eigenvalues and positive real part. Unstable node: real positive eigenvalues. Stable focus: complex eigenvalues and negative real part. Saddle node: real eigenvalues and different signs.

Let's study what happens near V_1 and $I_{ext}^{(1)}$. According to the previous, if $V < V_1$, we have a stable focus and for $V > V_1$ we have an unstable focus, so the equilibrium goes from stable to unstable when the voltage membrane is increased. We can see in figure 2.5 that when $I_{ext} < I_{ext}^{(1)}$ we have a spiral sink, i.e a stable focus, but when we increase the input, being $I_{ext} > I_{ext}^{(1)}$, we have the appearance of a stable limit cycle that has absorbed the stability of the fixed point, making it unstable. When it comes to neuronal dynamics, the stable focus in figure 2.5a corresponds to small damped oscillations or only one oscillation or action

potential. On the other hand, the limit cycle in figure 2.5b, corresponds to periodic spiking. To conclude, if we increase the applied intensity above $I_{ext}^{(1)}$, the system undergoes a supercritical Andronov-Hopf bifurcation, a stable limit cycle has appeared and the equilibrium point went from stable to unstable. In neuronal terms, we went from a single spike to a periodic spiking behaviour.

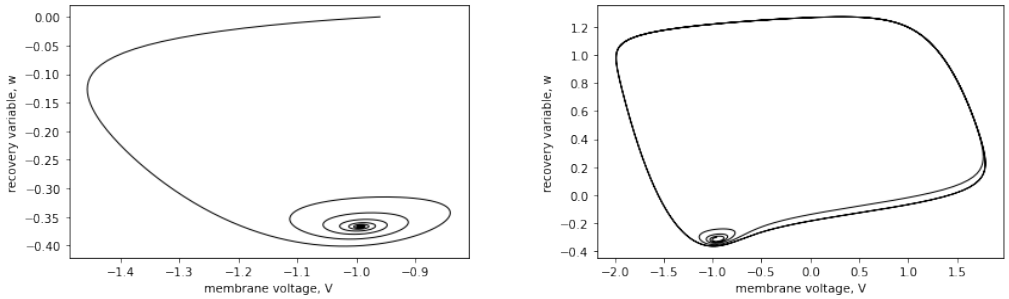

(a) Positive semi-orbit in system (2.11) when $I_{ext} = 0.30\mu A$ and the initial conditions are $(V_0, w_0) = (-0.96, -0.3)$.

(b) Positive semi-orbit in system (2.11) when $I_{ext} = 0.35\mu A$ and the initial conditions are $(V_0, w_0) = (-0.96, -0.3)$.

Figure 2.5: Phase plain before and after the Andronov-Hopf bifurcation. Figures obtained using the code taken from A.3 with $I_{ext} = 0.30 < I_{ext}^{(1)}$ and $I_{ext} = 0.35 > I_{ext}^{(1)}$, respectively.

Now, we are going to study what happens near V_2 and $I_{ext}^{(2)}$. If $V < V_2$, we have an unstable focus and if $V > V_2$, we have a stable focus. Hence, the equilibrium goes from unstable to stable when undergoes the Andronov-Hopf bifurcation. In figure 2.6a, we can see how initially we have a stable limit cycle and an unstable focus or a spiral source. The limit cycle collapses on the equilibrium point and we have a stable focus. It shrinks onto the equilibrium point, which absorbs the stability of the limit cycle and becomes stable, as we can see in figure 2.6b. We can see that if $I_{ext} > I_{ext}^{(2)}$, we stop the periodicity spiking and we have only damped oscillations or only one action potential or spike. The system undergoes a subcritical Andronov-Hopf bifurcation, leading to the disappearance of an attractor limit cycle that surrounds an unstable equilibrium point, which becomes stable after the bifurcation. From neuronal dynamics point of view, the neuron presented periodic spiking behaviour before the bifurcation and resting behaviour once the bifurcation occurred.

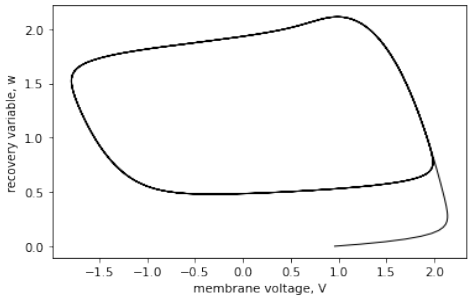

(a) Positive semi-orbit in system (2.11) when $I_{ext} = 1.40\mu A$ and the initial conditions are $(V_0, w_0) = (0.96, 0.3)$.

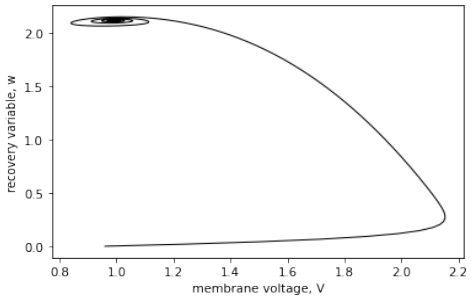

(b) Positive semi-orbit in system (2.11) when $I_{ext} = 1.45\mu A$ and the initial conditions are $(V_0, w_0) = (0.96, 0.3)$.

Figure 2.6: Phase plain before and after the bifurcation. Figures obtained using the code A.3 with $I_{ext} = 1.40 < I_{ext}^{(2)}$ and $I_{ext} = 1.45 > I_{ext}^{(2)}$, respectively.

FitzHugh-Nagumo model is not capable of generating bursting and chaos and does not take into account a lot of parameters, all the ionic currents have been underestimated. Given its dimension, it is not a used method when we want to study neurons with specific properties and cells that transmit a lot of information. Nevertheless, when it comes to action potential creation, the model showed the same kind of properties as the Hodgkin-Huxley. Moreover, as we have mentioned in section 2.1.1, the forced Van der Pol equation exhibits chaotic behaviour. Hence, there is also a modified FitzHugh-Nagumo Model, using the forced Van der Pol equations, that is capable of exhibiting bursting behaviour involving the sinus function.

Due to the importance of bursting in neuronal activity and transmission of information and since the FitzHugh-Nagumo model we analyzed is not capable of generating bursting, on the next chapter we are going to focus on bursting activity simulating some different types of bursting excitability.

Chapter 3

Bursting

When a neuron exhibits one single spike, less information is transmitted than when a neuron is capable of illustrating bursting behaviour, capable of illustrating a bunch of spikes and transmitting more information. Moreover, only a single spike is an inaccurate method of communication because it depends on a specific time. The spikes occur in a specific moment and just in that millisecond, another neuron has to perceive it and encode the information. Hence, spikes have a higher possibility of failing in crossing a synapse. Whereas on bursting behaviour, there is a higher possibility of crossing a synapse because the timing is not that specific. We have a bigger interval of spiking activity, having more time where the neuron can transmit information and interact with other neurons. In addition, bursting takes place in a lot of motor, sensory and cognitive brain behaviours and even in some diseases like epilepsy, making bursting an attractive aspect to study.

Definition 3.1. *Bursting is a dynamical phenomenon that occurs when a neuron fires repeatedly a group of spikes separated by a quiescent state, which can be resting or sub-threshold oscillations, creating a periodic loop that goes from resting to spiking. Each group of spikes is called a burst, a burst of two spikes is called a doublet, a burst of three spikes is called a triple and so on.*

Almost every neuron can burst if it is manipulated pharmacologically, stated in [23]. Hence, one can distinguish two different kinds of bursting: the forced one caused by a time-dependent input or the autonomous one when the neuron can burst on its own. Most excitable neurons are able to burst if we apply a current that slowly drives the neuron above and below the firing threshold. This slowly driving is related to the slow variable evolution of the slow subsystem. Moreover, bursting can occur due to the interaction of fast currents responsible for spiking activity and slow currents that modulate their activity, i.e. it can occur when we have a fast-slow system as in (2.9).

3.1 Fast-slow bursters

Fast-slow systems allow a description of this oscillatory behaviour based on two-time scales: one that modulates the fast dynamics and the other one that modulates the slow one, making small oscillations around the firing threshold and, in consequence, creating the bursting behaviour.

A fast-slow burster in $\mathbb{R}^n$ is a fast-slow system

$$\begin{aligned} \dot{x} &= f(x,u) \\ \dot{u} &= \epsilon g(x,u) \end{aligned} \tag{3.1}$$

where $x \in \mathbb{R}^m$ represents the fast-spiking behaviour, also called intraburst oscillation, and $u \in \mathbb{R}^{n-m}$ is a vector of parameters that represents the slow process that modulates x, called interburst oscillation. The variable u is called a quasistatic bifurcation parameter[1] and it depends on $x(t)$ and the parameter ϵ represents the small ratio of time scales between resting and spiking.

In bursting, we normally consider fast-slow bursters, where the slow variable u controls the spiking behaviour. If u goes through spiking and quiescent areas periodically, the neuron exhibits periodic bursting behaviour. Hence, the sustained bursting activity of the fast-slow system corresponds to the periodic activity of the reduced slow subsystem. The number of spikes in every burst is also controlled by u, because it depends on the time it spends on the spiking area.

In order to have bursting activity, the fast subsystem needs to be bistable, i.e. needs to have two different stable equilibrium states, the change from one state to the other is what creates the burst. That is why not all fast-slow systems are able to exhibit bursting, as we have seen in FitzHugh-Nagumo model in chapter 2, the fast subsystem must be complex enough to create bistability. In addition, there is the intuition that Hodgkin-Huxley model is a minimal model for bursting [2], so any model that is a strict simplification of it without any kind of modification is unable to burst. Hence, they invented qualitative models that have intrinsic mathematical interest in bursting but they are far from the biological behaviour of the

[1] The parameter changes slowly and with a constant rate.

[2] A minimal model for busting is a model that if we remove any current or gating variable, the system is unable to burst.

neuron, as we do not take into account currents of ions.

As bursting is described via a fast-slow system, it is studied dissecting the model making $\epsilon = 0$ and studying the fast and the slow subsystems separately. The goal is to study the fast subsystem and treat the other one as a vector of slowly changing bifurcation parameters.

Different phase plains configurations lead to different bursting activity. Commonly, the fast system has an attractor limit cycle for some values of the slow variable and an equilibrium attractor for other values of the slow variable, which means that the fast subsystem has an Andronov-Hopf bifurcation, seen in section 2.3.1.

Definition 3.2. *A burster is planar when the fast subsystem is a two-dimensional system.*

According to the dimension of the slow subsystem, we can have different types of bursting. We are going to focus on hysteresis loop periodic bursters. In this kind of bursting, quiescent state of x, pushes u outside the resting area and u goes through the spiking area, initiating the spiking activity after a while. Then, repetitive firing of x pushes u outside the spiking area going through the resting area and making the neuron rest. This previous process is repeated periodically creating bursting. The two stable equilibrium states co-exist for the same value of u on the fast subsystem, creating bistability of resting and spiking state. The former bistability is what creates a hysteresis loop. In this case, u can be one-dimensional.

When it comes to bursting, there are two important questions: what initiates sustained spiking during a burst and what terminates it temporally creating a quiescent state. Hence, the fast-slow bursters involve two different kinds of bifurcations: from a quiescent state to repetitive spiking and from repetitive spiking to a quiescent state. Switching between spiking and resting occurs because the slow variable drives the fast subsystem through a bifurcation, involving a stable equilibrium point and a stable limit cycle. According to that, the classification of different types of bursting is based on their bifurcation from one state to the other. Different types of bifurcations result in different topological types of bursting and the last one results in different neurocomputational properties. In addition, there are not only these two bifurcations, sometimes there is a bifurcation that leads to an increase of the membrane voltage but the neuron is not spiking yet, another bifurcation is needed in order to start the spiking behaviour, as we are going to see in some of the following examples.

We are going to focus on planar bursting and we are going to classify the different types of planar bursting and study some of them. We are going to make simulations of the bursting behaviour of both Morris-Lecar, see section 1.6, and Hindmarsh-Rose models, explained below. Classification is made based on the structure we have on the resting state and the quiescent area, we can have an equilibrium point, a limit cycle attractor, a torus... Hence, we can find the point-cycle, cycle-cycle, point-torus, cycle-torus, point-point and cycle-point bursters. Each one defines what exists in the quiescent state and what in the spiking state, being, for example, a point-cycle bursting when the quiescent state is a stable equilibrium point and the spiking state is a limit cycle attractor.

Gathering the bursting classification information from [7], in table 3.1 we summarize the different bifurcations that are responsible for creating planar bursting, being the first one the bifurcation that starts spiking activity and the second the one that ends spiking activity and starts the resting state. As mentioned before, the slow variable u plays the role of a bifurcation parameter and is considered to be one-dimensional in planar bursting. Hence, all the bifurcations mentioned in this table are of codimension 1.

fold/circle	**fold/homoclinic**	**fold/Hopf**	fold/fold cycle
circle/circle	circle/homoclinic	circle/Hopf	**circle/fold cycle**
Hopf/circle	**Hopf/homoclinic**	Hopf/Hopf	Hopf/fold cycle
subHopf/circle	**subHopf/homoclinic**	subHopf/Hopf	subHopf/fold cycle
fold cycle/circle	fold cycle/homoclinic	fold cycle/Hopf	fold cycle/fold cycle
homoclinic/circle	homoclinic/homoclinic	homoclinic/Hopf	homoclinic/fold cycle

Table 3.1: Classification of codimension 1 planar fast-slow bursters, i.e. fast-slow bursters being u in equation (3.1) a one-dimensional system. Hopf refers to supercritical Andronov-Hopf bifurcation, subHopf refers to subcritical Andronov-Hopf bifurcation, circle refers to saddle-node bifurcation on an invariant circle, fold cycle refers to fold limit cycle bifurcation and homoclinic refers to saddle homoclinic orbit bifurcation. Further information in [7].

We are going to study the planar bursters written in bold making simulations of them via Hindmarsh-Rose and Morris-Lecar models, and we are going to explain the necessary bifurcations in order to understand the examples illustrated in section 3.3.

3.2 Hindmarsh-Rose model

J. L. Hindmarsh and R. M. Rose[21] aimed to find a simpler model than Hodgkin and Huxley that exhibited rapid firing and bursting. The Hindmarsh-Rose remains one of the most popular mathematical models that describe qualitatively well the dynamics of a certain class of neuronal models using the Hodgkin-Huxley formalism.

As we have seen in chapter 2, FitzHugh-Nagumo model with the parameters I analyzed is not capable of bursting because there is no bistability, we have only one equilibrium point, see section 2.3 and equations (2.11). So we are going to introduce an attractive model capable of generating bursting behaviour. This model shows the transition between quiescence, tonic spiking and bursting, creating multi-stability regions using the proper parameter values.

Definition 3.3. *Tonic spiking is a kind of spiking activity that occurs at an elevated rate for an extended period of time but the number of spikes created is too low to be classified as a burst. Tonic spiking happens when the neuron exhibits regularly spaced spikes that are not considered bursting behaviour.*

3.2.1 Equations of the model

Hindmarsh and Rose proposed a three-dimensional Hindmarsh-Rose model in 1984[21] using the basis of the equations (2.10) of FitzHugh-Nagumo changing $g(x)$ for a quadratic function and adding a slow variable, z,

$$\begin{aligned} \dot{V} &= -aV^3 + bV^2 + w + I_{ext} - z, \\ \dot{w} &= c - dV^2 - \beta y, \\ \dot{z} &= \epsilon((V - V_0)s - z), \end{aligned} \tag{3.2}$$

where V is the membrane voltage and V_0 is the V-coordinate of the stable subthreshold equilibrium point in the case $I_{ext} = 0$, i.e. V_0 is the stable equilibrium of the resting state when no current is applied. In addition, w is the fast variable associated to the membrane recovery, i.e. channels that open during the action potential, and z is the slow variable that describes the activation or inactivation of some currents, having a rate of change of the order of ϵ. Moreover, a, b, c, s, β and ϵ are real constants, being $0 < \epsilon \ll 1$ the constant that bestows the slow dynamics.

Hindmarsh-Rose model, system (3.2), is a fast-slow subsystem having a two-dimensional fast subsystem with variables V and w, and a one-dimensional slow

subsystem when it comes to z. Moreover, system (3.2) becomes a fast-slow burster for some proper values of the parameters, as we will show in section 3.3. In consequence, this model is commonly used for its simplicity and its capacity of exhibiting bursting behaviour.

3.3 Planar point-cycle bursting

The goal of this section is to exhibit planar point-cycle bifurcations by doing simulations of Morris-Lecar and Hindmarsh-Rose model. As we have stated in section 1.6, Morris-Lecar model is really important because is the fast subsystem of a lot of fast-slow bursters. Hence, if we couple equations (1.10) with a linear slow subsystem, we are capable of exhibiting bursting behaviour, i.e. we are going to consider a system like

$$\begin{aligned} \dot{V} &= I(u) - g_L(V - E_L) - g_K w(V - E_K) - g_{Ca} m_\infty(V)(V - E_{Ca}), \\ \dot{w} &= \lambda(V)(w_\infty(V) - w), \\ \dot{u} &= \mu f(V), \end{aligned} \tag{3.3}$$

where u is the slow variable, $f(V)$ is a continuous function that we are going to consider lineal and $I(u)$ is the applied current, I_{ext}, that is a function of u. In the next section, we are going to see that for different values of μ, g_x and E_x for $x = K, Ca, L$, and different functions $f(V)$ and $I(u)$, system (3.3) shows different bursting behaviour.

We are going to study some kinds of bursting excitability and simulate them via Morris-Lecar or Hindmarsh-Rose model. We are going to study the different bifurcations that take place and we are going to study how the action potential behaves. In consequence, we are going to study time-voltage graphs indicating where each bifurcation occurs. The figures marked with an asterisk are from [7] and available on this website: Bursting excitability. Moreover, in the following time-voltage figures, fold holds for fold bifurcation, homo holds for saddle homoclinic orbit bifurcation, AH for Andronov-Hopf bifurcation, SNIC for saddle-node on invariant cycle bifurcation and cycle for fold limit cycle bifurcation.

3.3.1 Fold/homoclinic bursting (square-wave)

In this type of bursting, the resting state disappears via a fold bifurcation, so we are going to introduce it.

Fold bifurcation

A fold or saddle-node bifurcation occurs when two equilibrium points collide and annihilate each other or two equilibrium points are created, one that is a node and the other a saddle.

Definition 3.4. *Being*

$$\dot{x} = f(x, \alpha), x \in \mathbb{R}^n,$$

an autonomous system of ordinary differential equations and α our bifurcation parameter. The system undergoes a saddle-node bifurcation if we have two equilibrium points when $a < a_0$, one equilibrium point if $a = a_0$ and no equilibrium points if $a > a_0$. We could also have no equilibrium point, then only one and, in the end, two equilibrium points.

Theorem 3.5. *[27] (Saddle-Node bifurcation) Suppose $\dot{x} = f_\alpha(x) = f(x, \alpha)$ is a first-order differential equations for which*

1. $f_{\alpha_0}(\alpha_0) = 0$;
2. $f'_{\alpha_0}(x_0) = 0$;
3. $f''_{\alpha_0}(x_0) \neq 0$;
4. $\frac{\partial f_{\alpha_0}}{\partial \alpha}(x_0) \neq 0$.

Then this differential equation undergoes a saddle-node bifurcation at $\alpha = \alpha_0$

As we previously mentioned, the resting state disappears via a fold bifurcation, having two equilibrium points that collide and annihilate each other, leading to the appearance of the spiking period. In figure 3.1, we can see the two branches of each equilibrium point that has emerged. The branch located on the resting state corresponds to the attractor and the branch of the saddle is the one that has the limit cycle. We have an attractor equilibrium point at the resting state that via a fold bifurcation disappears and, as we have an attractor limit cycle on the spiking area, the spiking behaviour begins. As we can see in figure 3.1, there is not any limit cycle on the resting state, so there is not any kind of oscillations on the resting state. Once the neuron is on the spiking area, it goes on spiking until the homoclinic orbit bifurcation occurs, explained below, and the spiking disappears.

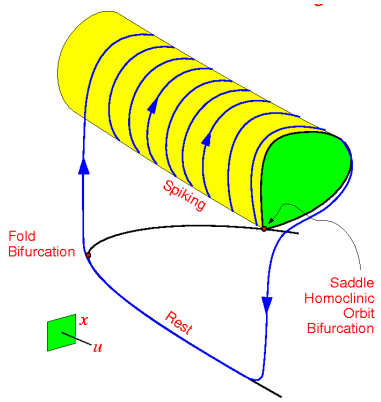

Figure 3.1: Fold/Homoclinic bursting via a fold/homoclinic hysteresis loop. Figure from [7]*.

Homoclinic orbit bifurcation

The homoclinic orbit bifurcation or saddle homoclinic orbit bifurcation occurs when the stable and unstable manifolds of the saddle surround an attractor limit cycle, see [20] where the former bifurcation is also called Andronov-Vitt bifurcation. We can see in figure 3.2a how the stable and unstable manifold of the saddle surrounds the limit cycle. This attractor limit cycle grows until it collides with the manifolds creating a homoclinic orbit to the saddle, see figure 3.2b. After the bifurcation, the limit cycle has disappeared and there is not any kind of attractor as depicted in figure 3.2c.

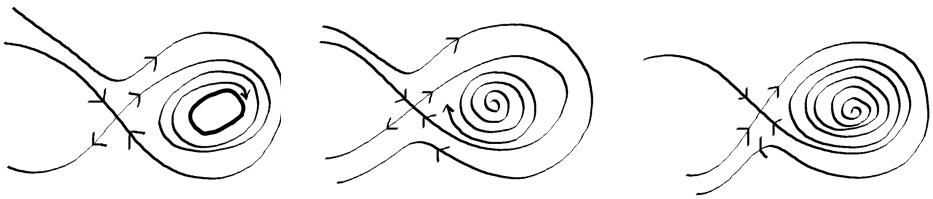

(a) (b) (c)

Figure 3.2: Phase plane of the system $\dot{x} = 2y$; $\dot{y} = 2x - 3x^2 + -y(x^3 - x^2 + y^2 - c)$, changing the bifurcation parameter c. Figure (a) is the phase plain of the previous system when $c = -0.1$. Figure (b) is the phase plain of the previous system when $c = 0$. Figure (c) is the phase plain of the previous system when $C = 0.1$. We can observe that when $c = 0$ the bifurcation occurs. Values of c taken from [26].

Once the system undergoes the homoclinic bifurcation, there is not any kind of attractor on the spiking state, what leads to the end of the spiking activity since we have a stable node on the resting state. The system goes back to the resting state because we have a stable equilibrium point there.

In figure 3.3, we simulated this type of bursting on Morris-Lecar and Hindmarsh-Rose model and indicated where each bifurcation takes place. We can observe that both models generated the same actions potentials behaviours qualitatively. As we mentioned previously, the spiking activity begins when the system undergoes a fold bifurcation and it ends when the system undergoes a homoclinic bifurcation.

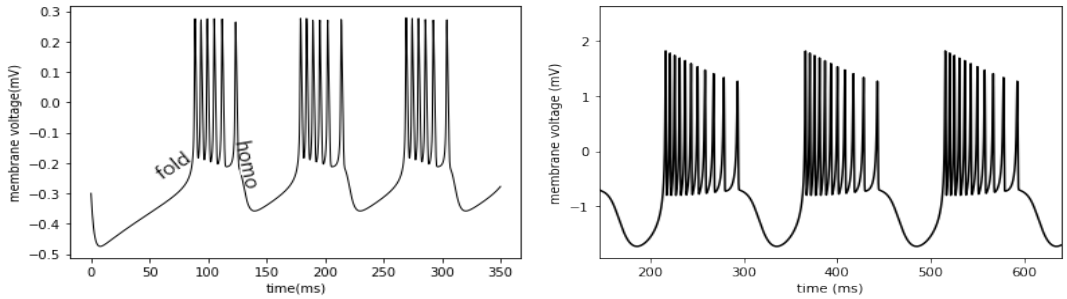

(a) (b)

Figure 3.3: (a): Time-voltage graph of the Fold/homoclinic bursting. Figure obtained using the code from A.4.3 using Morris-Lecar model with an intensity function $I(u) = -u$ and parameters $(V_1, V_2, V_3, V_4, E_L, E_K, E_{Ca}, g_L, g_K, g_{Ca}) = (-0.01, 0.15, 0.1, 0.05, -0.5, -0.7, 1, 0.5, 2, 1.2)$ in equations (1.10) and (1.11) and $\mu = 0.005$ in slow subsystem (3.3), see [7].
(b): Fold/homoclinic bursting behaviour in the Hindmarsh-Rose model, equations (3.2) with parameters $(I_{ext}, a, b, c, d, s, \epsilon, \beta, V_0) = (4, 1, 2.7, 1, 5, 4, 0.01, -1.6)$, following [14] and using the code in A.4.1.

3.3.2 Fold/Hopf bursting (tapered)

In this kind of bursting, the rest state disappears via a fold bifurcation, seen in the previous section, and the periodic limit cycle disappears via a supercritical Andronov-Hopf bifurcation, explained in section 2.3.1. Hence, after the Hopf bifurcation, the fixed point that remains is still stable, so in order to go to the resting state, another bifurcation is needed. The previous equilibrium point needs to become unstable in order to go to the resting state and to create bursting. In figure 3.4, this extra bifurcation is the fold one but we could have another kind of bifurcation. Hence, there are different kinds of hysteresis loops that can lead to that same kind of bursting. Moreover, in figure 3.4 the fast subsystem under-

goes two bifurcations while being excited: one corresponds to the termination of repetitive spiking and the other corresponds to the transition from the excited equilibrium point to resting via a saddle-node or a fold bifurcation. The supercritical Andronov-Hopf bifurcation ends the oscillations and the fold bifurcation sends the neuron to the resting state annihilating the stable equilibrium point. The first bifurcation determines the topological type of bursting and the second one is essential for determining the type of hysteresis loop. In addition, in figure 3.4 we can see how the branch of the saddle of the resting state connects with the branch of the saddle of the spiking state, the two branches of the saddle point on both fold bifurcations connect.

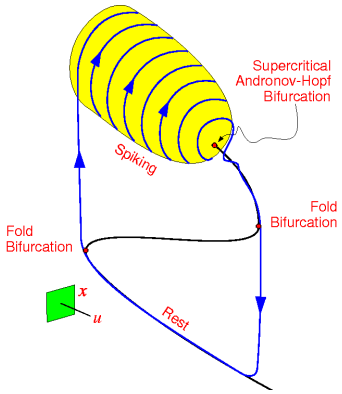

Figure 3.4: Fold/Hopf bursting via fold/fold hysteresis loop. Figure from [7]*.

In figure 3.5, we displayed this kind of bursting in Hindmarsh-Rose model, see section 3.2, and we can see how it goes vertically to spiking and that the amplitude of the action potential decreases(in a square root shape) as we approach the supercritical Hopf bifurcation. In this process, the limit circle shrinks causing each time a lower amplitude oscillation in the voltage. As we have stated before, the fold bifurcation starts the spiking behaviour, the membrane voltage oscillates until the Andronov-Hopf bifurcation occurs and the fold bifurcation sends the neuron back to the resting state creating a loop that causes bursting.

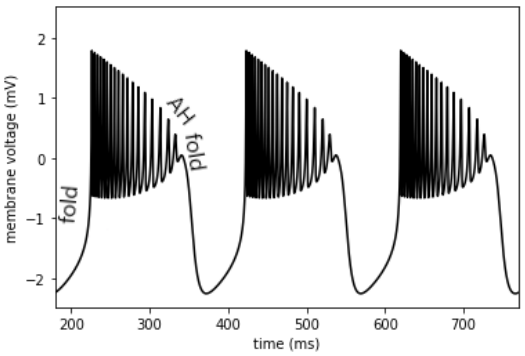

Figure 3.5: Fold/Hopf bursting behaviour in the Hindmarsh-Rose model, equations (3.2) with parameters $(I_{ext}, a, b, c, d, s, \epsilon, \beta, V_0) = (4, 1, 2.52, 1, 5, 4, 0.01, -1.6)$, following [14] and using the code in A.4.1.

3.3.3 Circle/Fold cycle bursting

In this kind of bursting, the spiking behaviour initiates via a saddle-node on invariant circle bifurcation, having previously a fold bifurcation, explained in section 3.3.1, or a subcritical Andronov-Hopf bifurcation, see section 2.3.1, which ends the resting state. Moreover, the spiking state disappears via a fold limit cycle bifurcation. The fold limit cycle bifurcation is the appearance or disappearance of two limit cycles, one stable and the other unstable.

Saddle-node on invariant circle bifurcation

The saddle-node on invariant circle bifurcation is a fold bifurcation that takes place in an invariant circle. On the one hand, the saddle and the node are connected by a heteroclinic orbit and the fold bifurcation occurs there, the two points shrink and we have a homoclinic orbit. Nevertheless, we can also have a limit cycle where a saddle and an attractor node emerge.

The appearance of a saddle and an attractor node is displayed in figure 3.6. In figure 3.6a, we have a limit cycle and in figure 3.6c we have an attractor node and a saddle-node that have emerged from a limit cycle.

This kind of bursting can be created via two different kinds of hysteresis loop: fold/fold cycle hysteresis loop, depicted in figure 3.7a, and a subHopf/fold cycle hysteresis, where there is a coexistence of resting and spiking states, depicted in figure 3.7b.

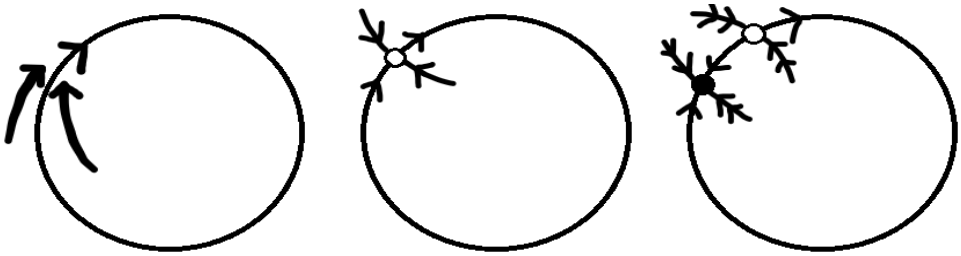

(a) Before the bifurcation. (b) During the bifurcation (c) After the bifurcation.

Figure 3.6: Phase plane of the saddle-node on invariant circle bifurcation. Two equilibrium points emerge from a limit cycle.

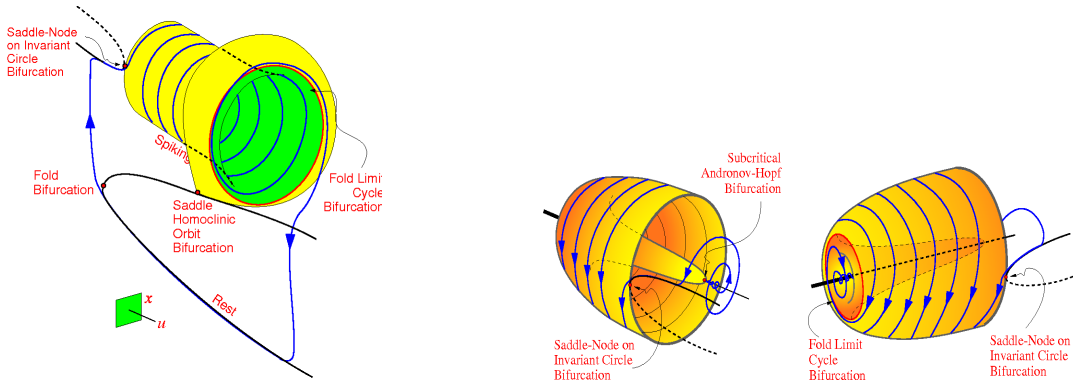

(a) Circle/Fold Cycle bursting via Fold/Fold Cycle hysteresis loop.

(b) Circle/Fold Cycle bursting via subHopf/Fold Cycle hysteresis loop.

Figure 3.7: Circle/Fold Cycle bursting. Figures from [7]*.

Concerning figure 3.7a, probably there might be parameters with which the system describes this type of bursting behaviour via a fold/fold cycle hysteresis loop. Nevertheless, we are going to focus on figure 3.7b and we are going to display its bursting behaviour. In this kind of bursting, the membrane potential starts to increase via a saddle-node on invariant circle and the voltage starts to oscillate initiating the spiking behaviour because of the existence of the attractor limit cycle. It goes on spiking until it undergoes a fold limit cycle bifurcation and the limit cycle disappears. The membrane voltage keeps constant for a while because of the stable point until it reaches the subcritical Andronov-Hopf bifurcation and it becomes unstable. Then, the neuron goes back to rest because of the stable point located on the resting state and the loss of attraction on the spiking area, starting the whole process again.

When it comes to figure 3.8, we have made a simulation of the action potential behaviour on the subHopf/fold cycle hysteresis loop in Morris-Lecar model, see section 1.6. As we can see in the figure, at the end of the spiking period, there is a thoughtful decline in the amplitude of the action potential after the fold limit cycle bifurcation, increasing a little bit and going directly to rest once the subcritical Andronov-Hopf bifurcation has occurred.

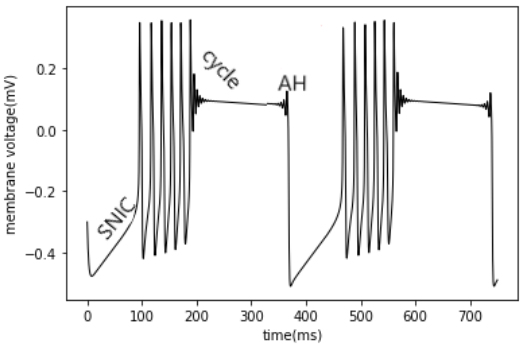

Figure 3.8: Time-voltage graphic of the Circle/Fold Cycle bursting via subHopf/Fold Cycle hysteresis loop. Figure obtained from the code in A.4.4 using Morris-Lecar model, equations (1.10) and (1.11), with intensity function $I(u) = -u$ and parameters $(V_1, V_2, V_3, V_4, E_L, E_K, E_{Ca}, g_L, g_k, g_{Ca}) = (-0.01, 0.15, 0.1, 0.16, -0.5, -0.7, 1, 0.5, 2, 1.36)$ coupled with the slow subsystem $\dot{u} = \mu(0.1 + V)$ with $\mu = 0.003$, see [7]*.

3.3.4 SubHopf/Homoclinic bursting

In this type of bursting, the quiescent state disappears via a subcritical Andronov-Hopf bifurcation, see section 2.3.1, and the spiking state disappears via a saddle homoclinic orbit bifurcation, explained in the previous section. We are going to focus on the bursting generated by a subHopf/homoclinic hysteresis loop.

The stable equilibrium point on the resting state disappears via a fold bifurcation and we jump on the attractor equilibrium point of the upstate, having an increase on the membrane voltage but the spiking activity has not started yet. It is not until the fold limit cycle bifurcation that the neuron presents spikes. As a stable limit cycle has appeared via the previous bifurcation, the neuron starts to generate action potentials that are lower every time because of the subcritical Andronov-Hopf bifurcation. Once the Andronov-Hopf bifurcation has occurred, the equilibrium point is unstable so we go to the other attractor limit cycle that co-exists leading to a spiking activity again until the saddle homoclinic orbit bifurcation is reached. The homoclinic bifurcation leads to the disappearance of the

attractor limit cycle and the neuron goes back to rest because of the attractor on the resting state.

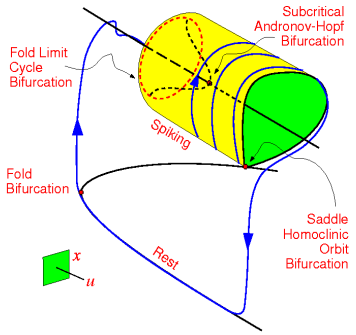

Figure 3.9: SubHopf/Homoclinic bursting via fold/homoclinic hysteresis loop. Figure from [7].

As we can see in figure 3.10, when the system undergoes the fold bifurcation the membrane voltage increases. The spiking behaviour starts because of the fold limit cycle bifurcation and the amplitude of the oscillations decreases because the system undergoes an Andronov-Hopf bifurcation. After the Hopf bifurcation, the point is unstable so the neuron starts to spike again because of the existence of an attractor limit cycle. The spiking behaviour stops when the system undergoes a saddle-homoclinic orbit bifurcation and the membrane voltage goes back to its resting value.

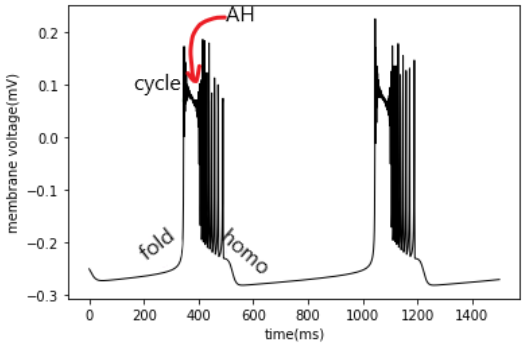

Figure 3.10: Time-voltage graph of subHopf/Homoclinic bursting. Figure taken from A.4.5 simulating the Morris-Lecar model, equations (1.10) and (1.11), with intensity function $I(u) = 0.08 - 0.03u$, voltage function $V_3(u) = 0.08 - u$ and parameters $(V_1, V_2, V_4, E_L, E_K, E_{Ca}, g_L, g_K, g_{Ca}) = (-0.01, 0.15, 0.04, -0.5, -0.7, 1, 0.5, 2, 0.9)$ coupled with the slow subsystem $\dot{u} = \mu(0.22 + V)$ where $\mu = 0.003$, following [7]*.

3.3.5 Hopf/homoclinic bursting

In this type of bursting, the quiescent state disappears via a supercritical Andronov-Hopf bifurcation, explained in section 2.3.1, and the periodic limit cycle attractor, corresponding to repetitive spiking, disappears via a saddle-node homoclinic bifurcation, see section 3.3.1.

Initially, the neuron is at the resting state and the resting equilibrium point is stable. So, as in all the previous examples, we have a fold bifurcation, see figure 3.11, and there is not any equilibrium point after it on the rest state and the neuron goes to the attractor point on the upstate. Hence, there is an increase in the membrane voltage but the neuron is not generating action potentials yet. Then, is when the supercritical Andronov-Hopf bifurcation starts the spiking behaviour because an attractor limit cycle is created. The neuron oscillates until the limit cycle disappears via a saddle homoclinic orbit bifurcation and it goes back to the stable equilibrium point on the resting state, creating a loop that generates this kind of bursting.

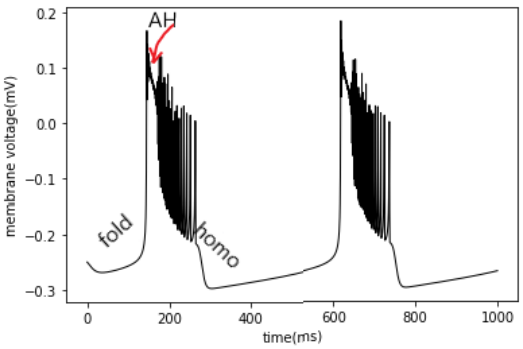

Figure 3.11: Time-voltage graph of Hopf/Homoclinic bursting via Fold/Homoclinic hysteresis loop. Figure obtained from the code in A.4.5 using Morris-Lecar model, equations (1.10) and (1.11), with intensity function $I(u) = 0.08 - 0.03u$, voltage function for the parameter V_3 $V_3(u) = 0.08 - u$ and parameters $(V_1, V_2, V_4, E_L, E_K, E_{Ca}, g_L, g_K, g_{Ca}) = (-0.01, 0.15, 0.02, 0.05, -0.5, -0.7, 1, 0.5, 2, 0.9)$ coupled with the slow subsystem $\dot{u} = \mu(0.22 + V)$ where $\mu = 0.01$, see [7].

Chapter 4

Conclusions and future work

4.1 Conclusions

We have studied the equations of Hodgkin-Huxley model understanding their origin and the different types of biological properties behind them. In addition, we understood the creation of an action potential and displayed a different kind of spiking behaviour on this model changing the applied current. We saw that we can go from one spike to periodic spiking and the other way around augmenting the applied current. In addition, we introduced Morris-Lecar model, a simplification of Hodgkin-Huxley model really important in fast-slow busters.

In the second chapter, we studied the origin of the FitzHugh-Nagumo equations and their periodicity behaviour when undergoing an Andronov-Hopf bifurcation. We saw how an Andronov-Hopf bifurcation takes an important role in the creation of periodicity behaviour with particular values of the parameters on the FitzHugh-Nagumo model.

Lastly, we focused on some of the different types of planar point-cycle bursting excitability describing the bifurcations that create it. We displayed the bursting behaviour simulating the Hindmarsh-Rose and Morris-Lecar model and we saw how different types of bifurcations lead to different types of bursting behaviours. Nevertheless, nowadays is not clear their biological consequence, we do not know the biological consequence if, for example, the resting state disappears via a fold bifurcation or a fold limit cycle bifurcation.

4.2 Future work

The following ideas could be considered in the future:

- It could be interesting to do simulations of bursting directly from Hodgkin-Huxley model, as done in [32], and compare them to the ones we obtained via simpler models.
- We could study the connection and the interaction of a net of neurons. There is a lot of research that studies the previous doing periodic perturbations, but it is not clear what kind of periodicity.
- Future research should consider different types of bursting, such as cycle-cycle bursting among others. In addition, we could consider other neuronal models than Morris-Lecar and Hindmarsh-Rose that display bursting behaviour, such as Wilson-Cowan, see [31], and Gavrilov-Shilnikov model, see [30].
- It would be interesting to study deeply the chaotic bursting behaviour such as the famous blue-sky catastrophe, seen in [7].
- We could also consider fast-slow bursters with two slow variables and study the different bursting behaviour they display.

Appendix A

Python's code

We did all the simulations in Google Colab and in Python. Moreover, we integrated the ordinary differential equations presented in this work with the odeint integrator, an integrator that uses the stepper algorithm Runge-Kutta4.

A.1 Hodgkin-Huxley model

```
import matplotlib.pyplot as plt
import math
import numpy as np

gl, gna, gk = 0.3, 120, 36 #we set the values of the constants
El, Ena, Ek = 10.6, 120, -12
C = 1

#equations of alpha and beta for initial values
V=[]
V.append(-70) #we initialize the initial constant values
#my initial voltage is -70
alpha_n = []
beta_n = []
alpha_m = []
beta_m = []
alpha_h = []
beta_h = []
alpha_n.append(0.01 * ( (10-V[0]) / (math.exp((10-V[0])/10) - 1)))
beta_n.append(0.125*math.exp(-V[0]/80))
alpha_m.append(0.1 * (25-V[0]) /(math.exp((25-V[0])/10)-1))
beta_m.append(4 * math.exp(-V[0]/18))
alpha_h.append(0.07 * math.exp(-V[0]/20))
beta_h.append(1 / (math.exp((30-V[0])/10)+1))
n = []
m = []
h = []
n.append(alpha_n[0]/(alpha_n[0] + beta_n[0])) #inital gate variables
m.append(alpha_m[0]/(alpha_m[0] + beta_m[0]))
```

```
h.append(alpha_h[0]/(alpha_h[0] + beta_h[0]))

#creat the time constants
time_total = 100
time_incr = 0.01
t = np.arange(0,time_total+time_incr, time_incr)
#t is our time vector
#we create our intensity vector
I=np.zeros(len(t)) #all 0's
I[:]=500 #we keep the applied current constant
#I kept changing this value
#observing the different kind of action potentials
for i in range(0, len(t)-1):
    #I apply the hh equations
    alpha_n.append(0.01*(10-V[i])/(np.exp((10-V[i])/10.0)-1))
    beta_n.append(0.125*np.exp(-V[i]/80.0))
    alpha_m.append(0.1 * ((25-V[i]) /(np.exp((25-V[i])/10.0)-1)))
    beta_m.append(4 * np.exp(-V[i]/18.0))
    alpha_h.append(0.07 * np.exp(-V[i]/20.0))
    beta_h.append(1 / (np.exp((30-V[i])/10.0)+1))


    Ina = gna*(m[i]**3)*h[i]*(V[i]-Ena);
    Ik = gk*(n[i]**4)*(V[i]-Ek)
    Il = gl*(V[i]-El)
    Iion = I[i] - Ina - Ik - Il

#I calculate the next values using the euler's first order aproximation
    V.append(V[i] + time_incr*Iion/C)
    n.append(n[i] + time_incr*(alpha_n[i]*(1-n[i])-beta_n[i]*n[i]))
    m.append(m[i] + time_incr*(alpha_m[i] *(1-m[i]) - beta_m[i] * m[i]))
    h.append(h[i] + time_incr*(alpha_h[i] *(1-h[i]) - beta_h[i] * h[i]))

plt.plot(t, V, color = "black", linewidth=1)
plt.xlabel("time (ms)")
plt.ylabel("Voltage (mV)")
plt.title("Voltage over time")

plt.plot(t, m, label = "m(t) K activation", color="blue", linewidth=1)
plt.plot(t, n, label ="n(t) Na activation", color="red", linewidth=1)
plt.plot(t, h, label="h(t) Na inactivation", color="black", linewidth=1)
plt.xlabel("time (ms)")
plt.ylabel("m, n and h")
plt.legend()
plt.title("activation or inactivation gating variables")
```

A.2 Forced Van der Pol oscillator

```
import matplotlib.pyplot as plt
import math
import numpy as np
from scipy.integrate import odeint

```

```
w=2*math.pi/10
def model(z, t):
  mu, A = 7.48, 1.05
  x, y = z
  dxdt = y
  dydt = mu*(1-x**2)*y-x+A*math.sin(w*t)
  dzdt= [dxdt, dydt]
  return dzdt
print(2*math.pi/w)
t = [i for i in range(10001)] #an array of time
z0=[0, 0]
sol = odeint(model, z0, t)
plt.figure(figsize=(15,4)) #I want a rectangular graph
for k in range(1, 1001):
  plt.scatter(sol[k*10,0], sol[k*10,1], color="black")
plt.xlabel("x")
plt.ylabel("y=dx/dt")
```

A.3 FitzHugh-Nagumo model

Python code that computed the solutions of the equation (2.11):

```
import matplotlib.pyplot as plt
import numpy as np
from scipy.integrate import odeint

def model(z, t): #time not used, is an autonomous system
  I=0.35 #the parameter I keep on changing.
  v, w = z
  dzdt = [v - (v**3)/3 - w + I, 0.08*(v+0.7-0.8*w)] #equations of the model
  return dzdt

t = np.linspace(0, 200, 1500) #an array of time
z0 = [-0.96, -0.3] #initial conditions
sol = odeint(model, z0, t)
plt.plot(sol[:, 0], sol[:, 1], color="black", linewidth=1)
plt.xlabel("membrane␣voltage,␣V")
plt.ylabel("recovery␣variable,␣w")
```

A.4 Bursting excitability

A.4.1 Simulation of bursting in Hindmarsh-Rose

```
import matplotlib.pyplot as plt
import math
import numpy as np
from scipy.integrate import odeint

def model(x, t):
  Iext = 4
  a, c, d, s, beta, v0, e = 1, 1, 5, 4, 1, -1.6, 0.01
```

```
  b = 2.52 #the parameter I change
  V, w, z = x
  dvdt = -a*V**3 + b*V**2 + w + Iext - z
  dwdt = c - d*V**2 - beta*w
  dzdt = e*(s*(V-v0)-z)
  dxdt = [dvdt, dwdt, dzdt]
  return dxdt

t = np.linspace(0,900, 15000)
x0 = [-1, 0, 0] #our model is insensitive to changes on the initial values.
sol = odeint(model, x0, t)
plt.xlabel("time (ms)")
plt.ylabel("membrane voltage (mV)")
plt.plot(t, sol[:, 0], "black")
plt.xlim(180, 770)
 #If I scale the x-axis like this the bursting behaviour is clearly observed.
```

A.4.2 SubHopf/homoclinic bursting

```
import matplotlib.pyplot as plt
import math
import numpy as np
from scipy.integrate import odeint
def minf(V, V1, V2):
  return (1/2)*(1+math.tanh((V-V1)/V2))

def winf(V, V3, V4):
  return (1/2)*(1+math.tanh((V-V3)/V4))

def landa(V, V3, V4):
  return (1/3)*math.cosh((V-V3)/(2*V4))

def model(z, t):
  #we define the different parameters
  #this is what we keep changing
  El, Ek, Eca = -0.5, -0.7, 1
  gl, gk, gca = 0.5, 2, 0.9
  mu = 0.003
  v1, v2, v4 = -0.01, 0.15, 0.04
  v, w, u = z
  #in this bursting V3 is a function of u
  dzdt = [0.08-0.03*u-gl*(v-El)-gk*w*(v-Ek)-gca*minf(v, v1, v2)*(v-Eca),
  landa(v, 0.08-u, v4)*(winf(v, 0.08-u, v4)-w), mu*(0.22+v)]
  #in the partial of the membrane voltage the intensity is I(u) = -u
  return dzdt

t = np.linspace(0,1500, 1500)
z0 = -0.25, 0, 0
sol = odeint(model, z0, t)
plt. plot(t, sol[:, 0], color = "black", linewidth=1)
plt.xlabel("time(ms)")
plt.ylabel("membrane voltage(mV)")
```

A.4.3 Fold/homoclinic bursting

```
import matplotlib.pyplot as plt
import math
import numpy as np
from scipy.integrate import odeint
def minf(V, V1, V2):
  return (1/2)*(1+math.tanh((V-V1)/V2))

def winf(V, V3, V4):
  return (1/2)*(1+math.tanh((V-V3)/V4))

def landa(V, V3, V4):
  return (1/3)*math.cosh((V-V3)/(2*V4))

def model(z, t):
  #we define the different parameters
  #this is what we keep changing
  El, Ek, Eca = -0.5, -0.7, 1
  gl, gk, gca = 0.5, 2, 1.2
  mu = 0.005
  v1, v2, v3, v4 = -0.01, 0.15, 0.1, 0.05
  v, w, u = z
  dzdt = [-u-gl*(v-El)-gk*w*(v-Ek)-gca*minf(v, v1, v2)*(v-Eca),
  landa(v, v3, v4)*(winf(v, v3, v4)-w), mu*(0.2+v)]
  #in the partial of the membrane voltage the intensity is I(u) = -u
  return dzdt

t = np.linspace(0,350, 1500)
z0 = -0.3, 0, 0
sol = odeint(model, z0, t)
plt. plot(t, sol[:, 0], color = "black", linewidth=1)
plt.xlabel("time(ms)")
plt.ylabel("membrane voltage(mV)")
```

A.4.4 Circle/fold circle bursting

```
import matplotlib.pyplot as plt
import math
import numpy as np
from scipy.integrate import odeint
def minf(V, V1, V2):
  return (1/2)*(1+math.tanh((V-V1)/V2))

def winf(V, V3, V4):
  return (1/2)*(1+math.tanh((V-V3)/V4))

def landa(V, V3, V4):
  return (1/3)*math.cosh((V-V3)/(2*V4))

def model(z, t):
  #we define the different parameters
  #this is what we keep changing
  El, Ek, Eca = -0.5, -0.7, 1
```

```
  gl, gk, gca = 0.5, 2, 1.36
  mu = 0.003
  v1, v2, v3, v4 = -0.01, 0.15, 0.1, 0.16
  v, w, u = z
  dzdt = [-u-gl*(v-El)-gk*w*(v-Ek)-gca*minf(v, v1, v2)*(v-Eca),              landa(v, v3, v4)*(win
  #in the partial of the membrane voltage the intensity is I(u) = -u
  return dzdt

t = np.linspace(0,750, 1500)
z0 = -0.3, 0, 0
sol = odeint(model, z0, t)
plt. plot(t, sol[:, 0], color = "black", linewidth=1)
plt.xlabel("time(ms)")
plt.ylabel("membrane voltage(mV)")
```

A.4.5 Hopf/homoclinic bursting

```
import matplotlib.pyplot as plt
import math
import numpy as np
from scipy.integrate import odeint
def minf(V, V1, V2):
  return (1/2)*(1+math.tanh((V-V1)/V2))

def winf(V, V3, V4):
  return (1/2)*(1+math.tanh((V-V3)/V4))

def landa(V, V3, V4):
  return (1/3)*math.cosh((V-V3)/(2*V4))

def model(z, t):
  #we define the different parameters
  #this is what we keep changing
  El, Ek, Eca = -0.5, -0.7, 1
  gl, gk, gca = 0.5, 2, 0.9
  mu = 0.01
  v1, v2, v4 = -0.01, 0.15, 0.02
  v, w, u = z
  #in this bursting V3 is a function of u
  dzdt = [0.08-0.03*u-gl*(v-El)-gk*w*(v-Ek)-gca*minf(v, v1, v2)*(v-Eca),
  landa(v, 0.08-u, v4)*(winf(v, 0.08-u, v4)-w), mu*(0.22+v)]
  #in the partial of the membrane voltage the intensity is I(u) = -u
  return dzdt

t = np.linspace(0,1000, 1500)
z0 = -0.25, 0, 0
sol = odeint(model, z0, t)
plt. plot(t, sol[:, 0], color = "black", linewidth=1)
plt.xlabel("time(ms)")
plt.ylabel("membrane voltage(mV)")
```

Bibliography

[1] A. L. Hodgkin and A. F. Huxley, *A Quantitative description of membrane current and its application to conduction and excitation in nerve*, *From the Physiological Laboratory, University of Cambridge*, (1952), 500–544.

[2] K. L. Anderson, J. Chism, Q. Hale, P. Klockenkemper, C. Pinkett, C. Smith and Dr. D. Badamdorj, *Mathematical Modeling Action Potential in Cell Processes*, (2013).

[3] M. Nelson and J. Rinzel, *Chapter 4: The Hodgkin-Huxley Model from The Genesis*, (2003).

[4] E. M. Izhikevich, *Dynamical Systems in Neuroscience: The Geometry of Excitability and Burstings*, (2007).

[5] R. Zillmer,, *Simple Neuron Models: FiftzHugh-Nagumo and Hindmarsh-Rose*, INF, Sezione di Firenze.

[6] A. Shilnikov and M. Kolomiets", *International Journal of Bifurcation and Chaos. Methods of the qualitative theory for the Hindmarsh-Rose Model: A case study. A tutorial*, V̲ol 18, (2008)

[7] E. M. Izhikevich, *Neural excitability, spiking and bursting*, International Journal of Bifurcation and Chaos, V̲ol 10, 1171-1266, (1999)

[8] E. M. Izhikevich, *bursting*, http://www.scholarpedia.org/article/Bursting, (2006)

[9] G. Huguet, *Introduction to mathematical neuroscience. International School. Dynamical Systems and applications*, Lecture 1, 2, 3 and 4, Brasil, (2021)

[10] P. Eckhoff and P. Holmes with contributions by K.Sadeghi, M. Schwemmer and K. Wong-Lin, *A short course in Mathematical Neuroscience*, Program in Applied and Computational Mathematics, Princeon University, (2015).

[11] T. Kanamaru, *Van der Pol oscillator*, Scholarpedia, http://www.scholarpedia.org/article/Van_der_Pol_oscillato, (2007)

[12] J. Guckenheimer and P. Holmes, *Nonlinear Oscillations, Dynamical Systems, and Bifurcations of Vector Fields*, (2002)

[13] W. Jiang and J. Wei, *Bifurcation analysis in van der Pol's oscillator with delayed feedback*, Department of Mathematics, Harbin Institute of Technology, (2006).

[14] R. Barrio and A. Shilnikov, *Parameter-sweeping techniques for temporal dynamics of neuronal systems: case study of Hindmarsh-Rose model*, Journal of Mathematical Neuroscience, (2011).

[15] G. Innocenti and R. Genesio, *On the dynamics of chaotic spiking-bursting transition in the Hindmarsh-Rose neuron.* Chaos 19, (2009)

[16] A.L. Hodgkin and A.F. Huxley, *A Quantitative Description of Membrane Current and its Application to Conduction and Excitation in Nerve.*, J Physil. 117, 500-544, (1952).

[17] C. Morris and H. Lecar, *Voltage oscillations in the barnacle giant muscle fiber.*, Laboratory of biophysics, (1981).

[18] A. Palit and D. P. Datta, *On the determination of exact number of limit cycles in Lienard Systems*, University of North Bengal, (2010).

[19] W. Gerstner, W. M. Kistler, R. Naud and L.Paninsky, *Neuronal Dynamics: From single neurons to networks and models of cognition*, (2014).

[20] S. V. Gonchenko, C. Simó and A. Vieiro, *Richness of dynamics and global bifurcations in systems with a homoclinic figure-eight*, (2012).

[21] J. L. Hindmarsh and R. M. Rose, *A model of neuronal bursting using three coupled first order differential equations*, 221:87-102, (1084).

[22] J. L. Hindmarsh and R. M. Rose, *A model of the nerve impulse using two first-order differential equations*, Nature, 269:162-164, (1982).

[23] F. Zeldenrust, W. J. Wadman and B. Englitz, *Neural coding with bursts-Current state and future perspectives*, Department of Neurophysiology, Radboud University, (2018).

[24] B. Hille, *Ion Channels of Excitable Membranes*, 1-22, (2001).

[25] J. M. Sotomayor, *Lições de equações diferenciais ordinárias*, (1979).

[26] J. K. Hale and H. Koçak, *Dynamics and Bifurcations*, (1996).

[27] M. W. Hirsch, S. Smale and R. L. Devaney, *Differential Equations, Dynamical Systems and An Introduction to Chaos*, (2004).

[28] K. T. Alligood, Tim D. Sauer and J. A. Yorke, *Chaos: An introduction to dynamical systems*, Springer, (1996).

[29] T. T. L. Wallace and L. T. H. Homer, *Mathematical Model of Forced Van Der Pol's Equations*, (2015).

[30] Y. Kuznetsov, *Elements of Applied Bifurcation Theory*, 2nd edition, (1995).

[31] H. R. Wilson and J. D. Cowan, *Excitatory and inhibitory interactions in localized populations of modeled neurons*, Biophysical Journal, 12, (1972).

[32] P. R. Shorten and D. J. N. Wall, *A Hodgkin-Huxley model exhibiting bursting oscillations*, (1999).